

# Optimal self-scheduling for a multi-energy virtual power plant providing energy and reserve services under a holistic market framework

Jian Wang<sup>a,b,\*</sup>, Valentin Ilea<sup>b</sup>, Cristian Bovo<sup>c</sup>, Ning Xie<sup>a</sup>, Yong Wang<sup>a</sup>

<sup>a</sup> Department of Electrical Engineering, Shanghai Jiao Tong University, Shanghai 200240, China

<sup>b</sup> Department of Energy, Politecnico di Milano, Milan 20156, Italy

<sup>c</sup> Department of Electrical, Computer and Biomedical Engineering, Università degli Studi di Pavia, Pavia 27100, Italy

## Abstract

This paper addresses a self-scheduling model for a multi-energy virtual power plant (MEVPP) to optimize its day-ahead energy and reserve schedules considering the participation in joint markets. The coordination of energy and reserve services is realized by developing a holistic market framework. MEVPP trades electric energy in day-ahead market and natural gas in natural gas market under the uniform price scheme. MEVPP provides reserve in ancillary service market under the pay-as-bid scheme considering uncertain market clearing prices. Reserve regulations are modeled for the reserve quality provided by MEVPP. MEVPP can sign contracts in capacity market for capacity adequacy. The electricity and natural gas imbalance payments and unsupplied reserve penalty resulting from uncertain PV generation are calculated in real-time. The case studies, based on the practical data from Italian power exchange and transmission system operator, show the economic achievements of MEVPP with multiple markets participation. The advantages of multi-energy coupling in improving flexibility and economic profit are numerically analyzed. MEVPP is proven to be a promising reserve service supplier for TSO. Because through reasonable regulations, the reserve quality of MEVPP can be improved with little impact on its total cost.

**Keywords:** multi-energy virtual power plant, aggregation, flexibility, ancillary service market, pay-as-bid, reserve regulation.

## Nomenclature

### Indices and sets

$vpp$	Index of MEVPP
$pv, chp, gb, ec, ac$ ( $DV$ )	Indices (set) of PV, CHP, GB, EC, and AC
$se, st, k$ ( $DS$ )	Indices (set) of SE, ST, and both SE and ST
$de, dc, dh$ ( $DM$ )	Indices (set) of DE, TCL, and DH
$u, d$	Indices of upward reserve and downward reserve
$t$	Index of time interval, from 1 to $N_t$
$\tau$ ( $H$ )	Index (set) of reserve remaining period
$w$ ( $W_u, W_d$ )	Index (sets) of strategies of upward reserve offers and downward reserve bids
$DA$ ( $T_{DA}$ )	Index (set) of day-ahead schedule
$RT$ ( $T_{RT}$ )	Index (set) of real-time schedule
$fu, fd$ ( $T_{final}$ )	Indices (set) of final dispatching when upward reserve is deployed, or downward reserve is deployed
$S1$ ( $T_{S1}$ )	Index (set) including day-ahead schedule, real-time schedule and final dispatching, $T_{S1} = T_{DA} \cup T_{RT} \cup T_{final}$
$S2$ ( $T_{S2}$ )	Index (set) including day-ahead schedule and real-time schedule, $T_{S2} = T_{DA} \cup T_{RT}$
$S3$ ( $T_{S3}$ )	Index (set) including real-time schedule and final dispatching, $T_{S3} = T_{RT} \cup T_{final}$

### Parameters

$\lambda_t^{DAM+}, \lambda_t^{DAM-}$	Electricity selling price and buying price in DAM (€/MWh)
$\lambda^{GM}$	Natural gas buying price in GM (€/MWh)
$\lambda_{t,w}^{ASM,u/d}, \sigma_{t,w}^{ASM,u/d}$	Price of upward/downward reserve in ASM (€/MWh), and the corresponding probability of being accepted (%)
$\chi_t^{u/d}$	Proportion of upward/downward reserve request from TSO (%)
$\lambda_t^{EIP+}, \lambda_t^{EIP-}$	Electricity imbalance payment prices of the withdrawal direction and injection direction (€/MWh)
$\lambda_t^{URP}$	Unsupplied reserve penalty price (€/MWh)
$\lambda^{GIP+}, \lambda^{GIP-}$	Natural gas imbalance payment prices of the injection direction and withdrawal direction (€/MWh)
$\rho_{chp}^{su/sd}$	Start-up/shut-down price of CHP (€)

$A_{vpp}^{DA,u/d}, A_{vpp}^{DA,u/d}$	Maximum and minimum offer/bid sizes of upward/downward reserve of MEVPP in ASM (MW)
$P_{vpp}^{CM}$	Capacity schedule from CM contract of MEVPP (MW)
$\eta_{chp}^{el/loss/hrs}$	Electricity production efficiency/heat loss coefficient/heat recovery efficiency of CHP
$\eta_{gb}$	Efficiency for heat production of GB
$COP_{ec/ac}$	Coefficient for the performance of EC/AC
$\eta_{se}^{ch/dch}, \eta_{st}^{ch/dch}$	Charging/discharging efficiencies of SE and ST
$P_{chp}, P_{chp}$	Maximum and minimum electrical power productions of CHP (MW)
$H_{gb}$	Maximum thermal power production of GB (MW)
$C_{ec/ac}$	Maximum cooling power production of EC/AC (MW)
$R_{chp}^{u/d}$	Ramp-up/ramp-down limit of CHP (MW)
$CAP_{se/st}$	Capacity of SE/ST (MWh)
$S_{se/st,t}^{ch/dch}, S_{se/st,t}^{ch/dch}$	Maximum and minimum charging/discharging powers of SE/ST (MW)
$SOC_{se/st}, SOC_{se/st}$	Maximum and minimum SOC of SE/ST
$P_{pv,t}^{DA}, \tilde{P}_{pv,t}^{RT,a}$	Day-ahead and real-time available PV capacities (MW)
$D_{de/dh,t}^{DA}$	Day-ahead demand of DE/DH (MW)
$D_{de,t}^m, D_{de,t}^p$	Maximum quantity of DE curtailment and increase (MW)
$\theta_{dc}^{S1}, \theta_{dc}^{S1}$	Maximum and minimum insensitive temperatures of TCL in $T_{S1}$ (°C)
$P_{vpp}^{CM}$	Contracted capacity quantity (MW)

27  
28

### Variables

$P_{vpp,t}^{S1}$	Electricity output of MEVPP in $T_{S1}$ (MW)
$P_{vpp,t}^{DA+}, P_{vpp,t}^{DA-}$	Electricity selling and buying quantities of MEVPP in DAM (MW)
$g_{vpp,t}^{S1}$	Natural gas consumption of MEVPP in $T_{S1}$ (MW)
$A_{vpp,t,w}^{DA,u/d}, A_{vpp,t}^{RT,u/d}$	Upward/downward reserves of MEVPP in day-ahead schedule and real-time schedule (MW)
$P_{vpp,t}^{EIP+}, P_{vpp,t}^{EIP-}$	Electricity imbalance of withdrawal and injection directions of MEVPP (MW)
$P_{vpp,t}^{URP,u/d}$	Unsupplied upward/downward reserve of MEVPP (MW)
$g_{vpp,t}^{GIP+}, g_{vpp,t}^{GIP-}$	Natural gas imbalance of injection and withdrawal directions of MEVPP (MW)
$P_{chp,t}^{S1}, h_{chp,t}^{S1}, g_{chp,t}^{S1}$	Electricity produced, heat produced, and natural gas consumed by CHP in $T_{S1}$ (MW)
$h_{gb,t}^{S1}, g_{gb,t}^{S1}$	Heat produced, and natural gas consumed by GB in $T_{S1}$ (MW)
$c_{ec,t}^{S1}, P_{ec,t}^{S1}$	Cooling produced, and electricity consumed by EC in $T_{S1}$ (MW)
$c_{ac,t}^{S1}, h_{ac,t}^{S1}$	Cooling produced and heat consumed by AC in $T_{S1}$ (MW)
$S_{se/st,t}^{S1,ch}, S_{se/st,t}^{S1,dch}$	Charging and discharging powers of SE/ST in $T_{S1}$ (MW)
$E_{se/st,t}^{S1}$	Energy stored in SE/ST in $T_{S1}$ (MWh)
$P_{pv,t}^{S1}$	Power output of PV generator in $T_{S1}$ (MW)
$d_{de,t}^{fu/fid,m}, d_{de,t}^{fu/fid,p}$	Curtailment and increase of DE in final dispatching when upward/downward reserve is deployed (MW)
$D_{de,t}^{S3}$	DE in $T_{S3}$ (MW)
$D_{de,t}^{S1}$	TCL in $T_{S1}$ (MW)
$\theta_{de,t}^{S1}$	Indoor temperature of TCL in $T_{S1}$ (°C)
$A_{pv/chp/se/ec/de,t}^{S2,u/d}$	Upward/downward reserve of PV/CHP/SE/EC/DE in $T_{S2}$ (MW)
$E_{se,t}^{S2,AS,u/d}$	Energy stored in SE considering the upward/downward reserve in $T_{S2}$ (MWh)
$I_{chp,t}^{DA}, I_{chp,t}^{DA,ss/d}$	On/off state and start-up/shut-down state of CHP

## 29 1. Introduction

30 In order to realize the global net zero target [1,2], large-scale fossil fuel power plants are being shut down and  
31 replaced by generation from renewable energy sources (RESs). However, fossil fuel power plants are the main  
32 source of flexibility for power system, on the contrary, RESs always introduce uncertainties caused by  
33 unpredictable weather changes [3,4]. Therefore, how to produce a reliable power supply with enough flexibility  
34 under high penetration of RESs has raised great interest.

35 [5,6] analyze different methods to characterize and enhance the flexibility of power system under high  
36 penetration of RESs. [7] evaluates the flexibility benefits of power system. In these studies, distributed energy  
37 resources (DERs) are always used to mitigate uncertainties through their flexible power supplies and to increase the  
38 flexibility of power system. However, DERs with small capacities cannot participate in the energy market or  
39 ancillary service market (ASM) alone according to the minimum capacity requirement stipulated by market rules  
40 [8,9]. [10] develops a blockchain-based TSO-DSO flexibility marketplace to help the trading of flexibility services  
41 amongst TSOs, DSOs, and small prosumers. Moreover, small-scale participants individually have very low  
42 influence on power system, while creating a huge computational complexity due to their large number. The  
43 aggregation service is therefore needed to gather the small-scale DERs as a single entity to reach the required  
44 capacity scale. For example, in Italy, the minimum offer/bid size for aggregators in ASM is set as 1 MW in Virtual  
45 Aggregated Mixed Unit (UVAM) project launched in 2018 [8,9,11,12].

46 Above all, the aggregation service is highly important in the current scenario mainly from two aspects. Firstly, it  
47 can mitigate the uncertainties resulting from RESs through flexible DERs and provide flexibility to help the  
48 operation of power system. Secondly, aggregation service can help small-scale DERs to participate in various  
49 markets and trade multiple services coordinately. Virtual power plant (VPP) is a virtual aggregator of various types  
50 of DERs to provide a reliable overall power supply/demand and takes part in different types of markets as a single  
51 entity [13,14]. The aggregated flexibility of VPP is evaluated in [15], considering the uncertainties of RESs.

52 The existing studies are rich in addressing the optimal self-scheduling problem of VPP in different types of  
53 markets. In [16], VPP optimally activates consumers in demand response programs to maximize its profit of trading  
54 energy in day-ahead market (DAM). In [17], VPP determines its schedule and trades energy and reserve in the  
55 DAM and ASM respectively, considering both decision-independent and decision-dependent uncertainties. [18]  
56 proposes a day-ahead self-scheduling model of VPP in energy market and reserve market, considering the  
57 uncertainties of renewable generations, market prices, electrical demands, and requests for reserve. [19] considers  
58 the optimal bidding strategy of VPP when providing frequency regulation services in ASM, limited by the battery  
59 cycle life. [20] extends the services of VPP to not only multiple markets (e.g. energy, reserve), but also multiple  
60 system services (e.g. fast frequency response, inertia, upstream reactive power), and local network services (e.g.  
61 voltage support).

62 All the studies above only consider the electricity carrier, however, the additional benefits from the coordination  
63 of multi-energy resources have not been addressed. The aggregation of multi-energy resources can further exploit  
64 economic revenues by increasing the energy utilization efficiency and enhancing the flexibility potential of VPP.  
65 Thus, [21] proposes a dynamic aggregation model to aggregate multiple types of distributed resources as a multi-  
66 energy VPP (MEVPP). In [22], a virtual smart energy hub (VSEH) is developed based on the energy hub and VPP.  
67 A two-stage model is proposed to optimize the operation of VSEH and transactions in day-ahead and intraday heat  
68 and power markets. [23] presents a risk-averse multi-objective method to tackle the self-scheduling problem of a  
69 virtual energy hub plant in the context of local energy markets. To maximize the revenue of energy and reserve  
70 transactions, [24] presents a two-stage stochastic optimization model for a multi-energy community under the  
71 uncertainty of reserve call, and [25] proposes a day-ahead scheduling model for an integrated community energy  
72 system in a joint energy market and ASM with the uncertainties of market prices and renewable generations. [26]  
73 focuses on the aggregation model for a MEVPP with multi-energy quick-start devices in both energy and reserve  
74 markets. In [27], the microgrid operator that manages the electrical and thermal energy supply makes decisions in  
75 the DAM and reserve market under the uncertainties of market prices. Thermostatically controlled load (TCL) is  
76 one of the important demand-side flexible resources in the multi-energy system. In [28], TCL provides intra-hour  
77 ancillary services with the contribution-based reward allocation mechanism presented.

78 The day-ahead optimal self-scheduling problem for VPP is typically a two-stage optimization problem [18,24,  
79 29-32]. The general idea is to view the optimal scheduling problem as the first stage, followed by the operational  
80 strategies in the second stage. The effects of uncertainties can be evaluated through various methods. In [29,33],  
81 stochastic programming (SP) is applied by generating scenarios to model different realizations of uncertainties. In  
82 [31], robust optimization (RO) is used to optimize the worst realization of uncertainties. [17] uses adaptive RO to  
83 avoid the over-conservativeness of RO. In [24,32], RO is used for uncertain market prices, whereas SP is used for  
84 uncertain RESs and energy demands.

85 Despite these comprehensive works, there still exist gaps that the present work seeks to fill:

- 86 (1) Although there exist works focusing on VPP in different types of markets, few of them present a holistic  
87 market framework. In [16,22,23], VPP only trades energy in the energy markets, mainly in DAM. In [19], VPP  
88 only trades frequency regulation service in ASM. In [17,18,20,25,26], both DAM and ASM are presented,  
89 however, without considering market or payment mechanism reflecting close to real-time conditions. [21]  
90 considers energy trading in DAM and imbalance payment in real-time, however, without participating in ASM.  
91 Therefore, the economic results of these works may not be reliable enough.
- 92 (2) Seldomly it is considered that various multi-energy devices can provide or help to provide reserve service. In  
93 [21-23], multi-energy devices only produce energy without considering reserve service. In [26], the reserve of  
94 MEVPP is deployed as a whole, without focusing on the technical limits of devices inside MEVPP. In [25] only  
95 gas turbines and in [27] only electrical energy storages and interruptible loads are considered to provide  
96 reserves. In [24], the reserves provided by various conversion devices, storages and flexible demands are  
97 focused on, however, the corresponding technical limits are not fully considered. For example, unit  
98 commitment and ramping limits for combined heat and power unit (CHP), state of charge (SOC) for battery  
99 energy store, et al, are neglected which may lead to unreliable reserve services. Moreover, renewable  
100 generators such as photovoltaic (PV) generators can also provide reserve services that are neglected. Therefore,  
101 the ability of MEVPP to provide reserve service needs to be further explored.
- 102 (3) The regulations for reserve service are neglected in most of the works. However, as in the official documents  
103 [8,9,11,12], the reserve regulations including minimum offer/bid size and minimum delivery duration need to  
104 be strictly followed by all aggregators to provide a certain quality of reserve service for power system security.  
105 In [17-20,24-27] although the reserve scheduling problem is analyzed, none of them considers the model of  
106 reserve regulations. Therefore, the reserve services in the existing works can be unreasonable.
- 107 (4) Most of the existing works about aggregators participating in various markets are based on the uniform price  
108 scheme, which is easy to be adapted by price takers because they can regard the forecasted market clearing  
109 prices as their own remuneration prices. Paper [16-27] set uniform price assumption in all market stages.  
110 However, there are countries using pay-as-bid scheme in certain market stages, such as ASM in Italy and  
111 Germany. In this situation, the methods in these works partially lose the reference value.

112 In this paper, an optimal energy and reserve scheduling problem for a MEVPP is proposed. Its participation in  
113 joint markets is considered based on the Italian market rules. But it can be easily adapted to other market rules. The  
114 contributions of this paper include:

- 115 (1) A holistic market framework is developed, under which MEVPP coordinately optimizes its day-ahead energy  
116 and reserve schedules considering the transactions in capacity market (CM), DAM, ASM and natural gas  
117 market (GM). Electricity imbalance payment (EIP), natural gas imbalance payment (GIP) and unsupplied  
118 reserve penalty (URP) are set close to real-time for penalizing the energy imbalance and reserve unsupplied  
119 caused by uncertainties. A RO model is formulated to deal with the uncertainties arising from PV capacity.
- 120 (2) The advantages of multi-energy coupling in increasing the energy utilization efficiency and improving the  
121 potential flexibility of MEVPP are analyzed by formulating the energy and reserve schedules of all multi-  
122 energy devices under the corresponding detailed technical constraints. The extra economic profit from multi-  
123 energy coupling is also numerically evaluated.
- 124 (3) To improve the practical significance, the impacts of reserve regulations, including minimum offer/bid size and  
125 minimum delivery duration, on the reserve quality of MEVPP are considered. Moreover, different price  
126 schemes are considered for different market stages. Uniform price scheme is used in DAM and GM while pay-  
127 as-bid scheme is used in ASM considering uncertain market clearing prices.

128 The remainder of the paper is organized as follows. In section 2, the holistic market framework and optimal self-  
129 scheduling model of MEVPP are built in section 2.1 and section 2.2, respectively, followed by the MEVPP  
130 structure described in section 2.3. The problem is linearized into mixed-integer linear programming (MILP) in  
131 section 2.4. Section 3 analyzes the case studies. Section 4 draws the conclusions.

## 132 **2. Problem description**

### 133 *2.1. Holistic market framework*

134 The structure of the problem is described in Fig.1. MEVPP optimizes its schedules in the decision-making layer  
135 considering the information received from the physical and market layers.

136 In CM, MEVPP signs annual/monthly capacity contracts with the transmission system operator (TSO) to offer a  
137 total quantity on DAM and ASM at certain hours (especially peak hours) of the day [34] to ensure the adequacy and  
138 reliability of electricity supply. The process of capacity optimization is not the focus of this paper; only the output is,

139 i.e. the contracted capacity. MEVPP makes its schedule considering the constraints about the contracted capacity  
 140 from CM.

141 DAM is organized by the market operator (MO), also called power exchange, on day D-1 (the day before the  
 142 delivery day, also called day-ahead stage). Uniform price scheme is applied in DAM. MEVPP does not directly  
 143 participate in DAM but responds to the prices as a price taker. Dual price mechanism is considered, which means  
 144 the price of buying electricity is higher than the price of selling electricity for MEVPP [9,35]. The day-ahead  
 145 energy schedule of MEVPP after DAM is set as the day-ahead baseline and sent to TSO. GM is organized by MO  
 146 on day D-1 which is also based on the uniform price scheme. MEVPP buys natural gas at this price.

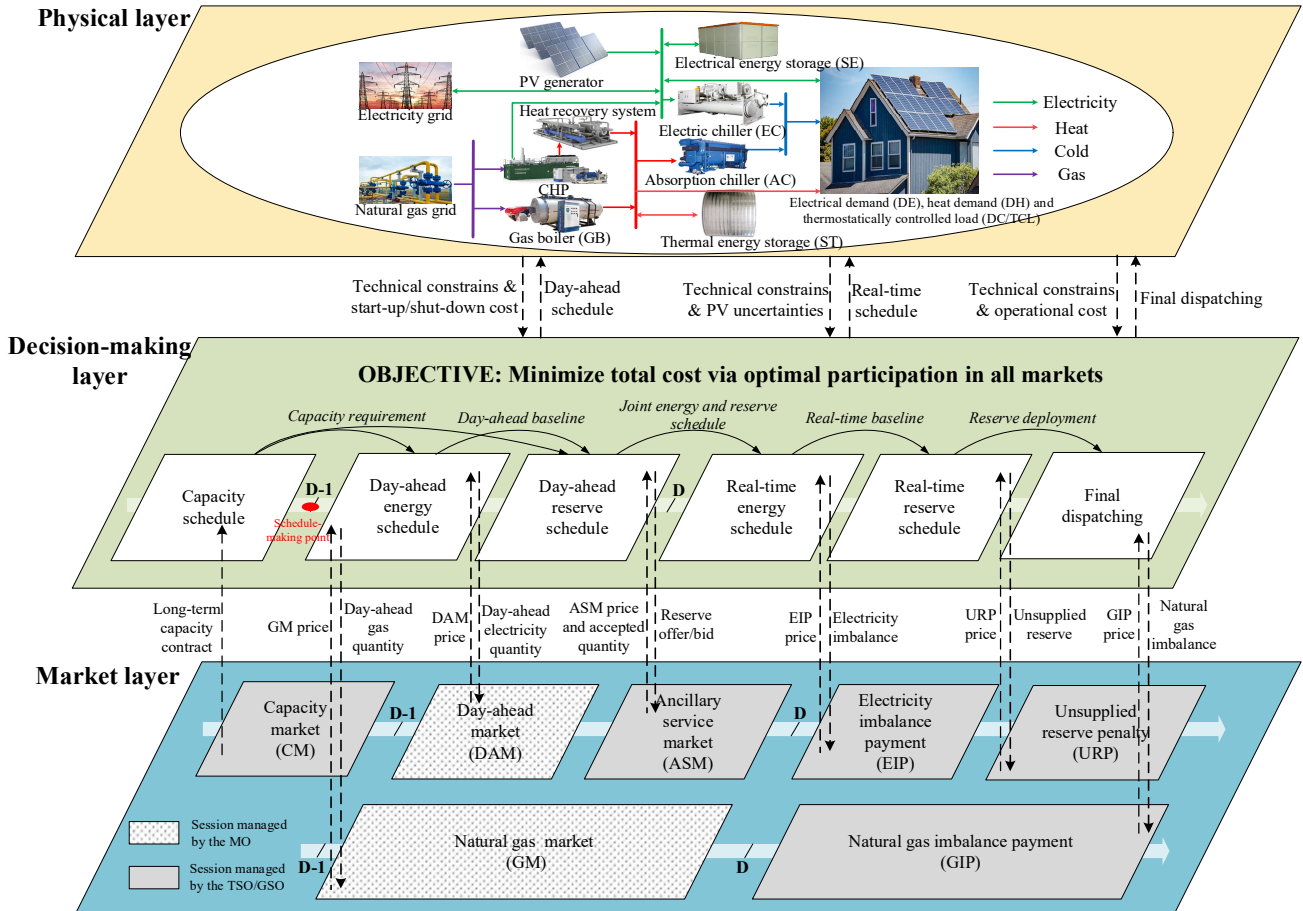


Fig.1 Structure of the self-scheduling problem of MEVPP under a holistic market framework

147  
 148  
 149  
 150

151 ASM is organized by TSO mainly to trade reserve services. According to the Italian market rules, MEVPP only  
 152 receives energy remuneration when the reserve band is deployed to energy produced/consumed in real time to help  
 153 TSO balance the power system. Moreover, ASM follows pay-as-bid scheme based on the economic merit order.  
 154 Therefore, MEVPP is remunerated according to the price it offers/bids when accepted by ASM.

155 On day D (the delivery day, also called real-time stage), the real-time energy schedule of MEVPP may be  
 156 different from the day-ahead energy schedule due to the uncertainties introduced, especially by RESs. This energy  
 157 deviation is penalized by EIP according to a settled imbalance cost.

158 TSO updates the day-ahead baseline to the real-time baseline according to the real-time energy schedule of  
 159 MEVPP and computes its reserve requirement. TSO checks if the reserve requirement can be technically supplied.  
 160 The unsupplied reserve is penalized in URP.

161 After the reserve deployment by TSO, MEVPP receives the final dispatching and calculates the operational costs  
 162 of all devices. GIP penalizes the natural gas deviation between the final dispatching and day-ahead energy schedule.

## 163 2.2. Optimal energy and reserve scheduling model of MEVPP

### 164 2.2.1 Objective function

165 The profit MEVPP earns in DAM is calculated by Eq.(1). The profit (negative cost) of MEVPP in GM for  
 166 buying natural gas is calculated by Eq.(2).  
 167

$$F_t^{DAM} = \lambda_t^{DAM+} \cdot p_{vpp,t}^{DA+} - \lambda_t^{DAM-} \cdot p_{vpp,t}^{DA-} \quad (1)$$

$$F_t^{GM} = -\lambda_t^{GM} \cdot g_{vpp,t}^{DA} \quad (2)$$

168 The market clearing prices of ASM are highly dependent on operational conditions and thus are subject to a high  
 169 degree of uncertainty and need to be modeled as such. According to the Italian market rules for aggregators [8, 9], a  
 170 MEVPP can offer/bid one pair of price-quantity at a time in the upward and/or downward direction in ASM and this  
 171 will be accepted or not depending on the market clearing price of the considered ASM session. Thus, considering as  
 172 an example the upward reserve,  $\rho_t^{ASM,u}$  is the market clearing price at time  $t$ , which is an uncertain variable  
 173 following the density function  $f_t^\rho : \mathbb{R} \rightarrow \mathbb{R}^+$ . Given a price-quantity offer at time  $t$ ,  $(\lambda_t^{ASM,u}, A_{vpp,t}^{DA,u})$ , its probability of  
 174 being accepted is computed as:

$$P[\rho_t^{ASM,u} \geq \lambda_t^{ASM,u}] = \int_{\lambda_t^{ASM,u}}^{\infty} f_t^\rho(l) dl \quad (3a)$$

175 where  $l$  is an auxiliary integration variable.

176 In practice, historical data must be used to obtain the continuous function  $f_t^\rho$ . However, ASM is strongly  
 177 dependent on real-time conditions, making the market clearing price difficult to characterize over long-term.  
 178 Therefore, only short-term historical data can be reliably used, and the data set is reduced. So it is more reasonable  
 179 to represent the market clearing price using a discrete set of possible values  $\{\rho_{t,n}^{ASM,u}, n = 1, \dots, N\}$ , where to each  
 180 possible price  $\rho_{t,n}^{ASM,u}$  a probability of realization  $\pi_{t,n}^{ASM,u}$  is associated such that  $\sum_n \pi_{t,n}^{ASM,u} = 1$ . Eq.(3a) becomes [36]:

$$\sigma_t^{ASM,u} = P[\rho_t^{ASM,u} \geq \lambda_t^{ASM,u}] = \sum_n M_{t,n}^u \cdot \pi_{t,n}^{ASM,u} \quad (3b)$$

181 where

$$M_{t,n}^u = \begin{cases} 1, & \rho_{t,n}^{ASM,u} \geq \lambda_t^{ASM,u} \\ 0, & \rho_{t,n}^{ASM,u} < \lambda_t^{ASM,u} \end{cases} \quad (3c)$$

182 If a pay-as-bid remuneration scheme is adopted, the expected remuneration price  $\lambda_t^{ASM,u*}$ , providing the MEVPP  
 183 offer is accepted, is [36]:

$$\mathbf{E}[\lambda_t^{ASM,u*} | \rho_t^{ASM,u} \geq \lambda_t^{ASM,u}] = \lambda_t^{ASM,u} \quad (3d)$$

184 Following [37], the expected return  $r$  of the MEVPP is:

$$\mathbf{E}[r] = P[\rho_t^{ASM,u} \geq \lambda_t^{ASM,u}] \cdot \mathbf{E}[\lambda_t^{ASM,u*} | \rho_t^{ASM,u} \geq \lambda_t^{ASM,u}] \cdot A_{vpp,t}^{DA,u} \quad (3e)$$

185 Substituting (3b) and (3d) into (3e) one gets:

$$\mathbf{E}[r] = \sigma_t^{ASM,u} \cdot \lambda_t^{ASM,u} \cdot A_{vpp,t}^{DA,u} \quad (3f)$$

186 Finally, considering several significant price offer strategies  $w(W_u)$  MEVPP can propose to ASM, MEVPP will  
 187 choose one strategy each time to maximize its expected profit. Therefore, the expected profit of MEVPP at time  $t$   
 188  $F_t^{ASM,u}$  is described by the following:

$$F_t^{ASM,u} = \sum_{w \in W_u} \sigma_{t,w}^{ASM,u} \cdot \lambda_{t,w}^{ASM,u} \cdot A_{vpp,t,w}^{DA,u} \quad (3g)$$

189 The downward reserve follows the same rule as the upward reserve but in the opposite direction. MEVPP needs  
 190 to give money back because when downward reserve is deployed, MEVPP can save the fuel cost and operational  
 191 cost from the decreased electricity production. Therefore, it is fair to return a part of the DAM remuneration.

$$F_t^{ASM,d} = \sum_{w \in W_d} \sigma_{t,w}^{ASM,d} \cdot \lambda_{t,w}^{ASM,d} \cdot A_{vpp,t,w}^{DA,d} \quad (3h)$$

192 where

$$\sigma_t^{ASM,d} = P[\rho_t^{ASM,d} \leq \lambda_t^{ASM,d}] = \sum_n M_{t,n}^d \cdot \pi_{t,n}^{ASM,d}$$

194 where

$$M_{t,n}^d = \begin{cases} 1, & \rho_{t,n}^{ASM,d} \leq \lambda_t^{ASM,d} \\ 0, & \rho_{t,n}^{ASM,d} > \lambda_t^{ASM,d} \end{cases}$$

195 Above all, the expected profit MEVPP earns in ASM is computed by Eq.(3). TSO either deploys upward or  
 196 downward reserve each time, which is represented by proportions  $\chi_t^u$  and  $\chi_t^d$ , summed up to 100%.

197

$$F_t^{ASM} = \chi_t^u \cdot F_t^{ASM,u} - \chi_t^d \cdot F_t^{ASM,d} = \chi_t^u \cdot \sum_{w \in W_u} \sigma_{t,w}^{ASM,u} \cdot \lambda_{t,w}^{ASM,u} \cdot A_{vpp,t,w}^{DA,u} - \chi_t^d \cdot \sum_{w \in W_d} \sigma_{t,w}^{ASM,d} \cdot \lambda_{t,w}^{ASM,d} \cdot A_{vpp,t,w}^{DA,d} \quad (3)$$

198

199

200

In day-ahead stage, the start-up/shut-down state of CHP is decided. The cost is calculated by Eq.(4):

$$CO_i^{sud} = \sum_{chp \in DV} \left( \rho_{chp}^{su} I_{chp,t}^{DA,su} + \rho_{chp}^{sd} I_{chp,t}^{DA,sd} \right) \quad (4)$$

201

202

The payment of electricity imbalance between real-time energy schedule and day-ahead energy schedule in EIP is calculated by Eq.(5).

$$F_t^{EIP} = -\lambda_t^{EIP+} \cdot p_{vpp,t}^{EIP+} + \lambda_t^{EIP-} \cdot p_{vpp,t}^{EIP-} \quad (5)$$

203

204

205

206

The unsupplied reserve, which is the difference between the reserve requirement from TSO and the real-time reserve schedule of MEVPP, is penalized in URP by Eq.(6).

$$F_t^{URP} = \lambda_t^{URP} \cdot p_{vpp,t}^{URP,u} + \lambda_t^{URP} \cdot p_{vpp,t}^{URP,d} \quad (6)$$

207

208

209

210

The natural gas imbalance payment in GIP is calculated by Eq.(7) for the natural gas deviation between final dispatching and day-ahead energy schedule.

$$F_t^{GIP} = \lambda_t^{GIP+} \cdot g_{vpp,t}^{GIP+} - \lambda_t^{GIP-} \cdot g_{vpp,t}^{GIP-} \quad (7)$$

211

212

213

214

215

To compute the net total cost of MEVPP, the accepted reserve is deployed to energy. The operational cost is calculated according to the final dispatching as is in Eq.(8), where  $co_i$  represents the operational costs of CHP, EC, PV, GB and AC.  $co_k$  represents the operational costs of SE and ST.  $co_j^m$ ,  $co_j^p$  are the costs of DE curtailment and increase.

$$CO_t^{op} = \sum_{\substack{i \in DV, \\ k \in DS, j \in DM}} \left[ \lambda_t^u \cdot \left( co_i \cdot p_{i,t}^{fiu} + co_k \cdot \left( s_{k,t}^{fiu,ch} + s_{k,t}^{fiu,dch} \right) + co_j^m \cdot d_{j,t}^{fiu,m} + co_j^p \cdot d_{j,t}^{fiu,p} \right) + \lambda_t^d \cdot \left( co_i \cdot p_{i,t}^{fid} + co_k \cdot \left( s_{k,t}^{fid,ch} + s_{k,t}^{fid,dch} \right) + co_j^m \cdot d_{j,t}^{fid,m} + co_j^p \cdot d_{j,t}^{fid,p} \right) \right] \quad (8)$$

216

217

218

219

The target of MEVPP is to minimize its total cost under the holistic market framework, which is described in the objective function Eq.(9). The time resolution of the whole optimization problem is 15 minutes.

$$\min \sum_{t \in T} \left( -F_t^{DAM} - F_t^{GM} - F_t^{ASM} + CO_t^{sud} + F_t^{EIP} + F_t^{URP} + F_t^{GIP} + CO_t^{op} \right) \quad (9)$$

220

221

## 2.2.2 Constraints of day-ahead energy schedule

222

223

224

225

226

227

228

Eq.(10) represents the power balance of MEVPP. The electricity withdraws (or exports) from and injects (or imports) to MEVPP are considered separately as in Eq.(11). Eq.(12) imposes that the electricity withdrawal and injection are positive and lower than the maximum limit  $\overline{P_{vpp}^{DA,s}}$  and  $\overline{P_{vpp}^{DA,b}}$ , respectively. The electricity withdrawal and injection are made complementary due to the cost minimization term of DAM in the objective function. Eq.(13) represents the natural gas balance. Eq.(14) limits that MEVPP can only buy natural gas under the maximum limit  $\overline{G_{vpp}^{DA}}$ . Eq.(15)-(16) represent the heat balance and cooling balance of MEVPP, respectively.

$$p_{vpp,t}^{DA} = \sum_{\substack{pv, chp, se, ec, \\ de \in DV \cup DS \cup DM}} \left( p_{pv,t}^{DA} + p_{chp,t}^{DA} + \left( s_{se,t}^{DA,dch} - s_{se,t}^{DA,ch} \right) - p_{ec,t}^{DA} - D_{de,t}^{DA} \right) \quad (10)$$

$$p_{vpp,t}^{DA+} - p_{vpp,t}^{DA-} = p_{vpp,t}^{DA} \quad (11)$$

$$\begin{cases} 0 \leq p_{vpp,t}^{DA+} \leq \overline{P_{vpp}^{DA,s}} \\ 0 \leq p_{vpp,t}^{DA-} \leq \overline{P_{vpp}^{DA,b}} \end{cases} \quad (12)$$

$$g_{vpp,t}^{DA} = \sum_{chp, gb \in DV} \left( g_{chp,t}^{DA} + g_{gb,t}^{DA} \right) \quad (13)$$

$$0 \leq g_{vpp,t}^{DA} \leq \overline{G_{vpp}^{DA}} \quad (14)$$

$$0 = \sum_{\substack{chp, gb, st, ac, \\ dh \in DV \cup DS \cup DM}} \left( -h_{chp,t}^{DA} - h_{gb,t}^{DA} - \left( s_{st,t}^{DA,dch} - s_{st,t}^{DA,ch} \right) + h_{ac,t}^{DA} + D_{dh,t}^{DA} \right) \quad (15)$$

$$0 = \sum_{ec,ac,dc \in DV \cup DM} (-c_{ec,t}^{DA} - c_{ac,t}^{DA} + D_{dc,t}^{DA}) \quad (16)$$

229 The time interval of this paper is 15 minutes, corresponding to ASM clearing time. However, in general, DAM  
 230 and GM consider time intervals longer than ASM. In Italy, ASM clears every 15 minutes while DAM and GM clear  
 231 every hour. Therefore, the variables in day-ahead energy schedule need to follow Eq.(17):

$$z_t^{DA} = z_{t'}^{DA}, \quad \forall t, t' \in Q_{hr} \quad (17)$$

232 where  $Q_{hr}$  is the set of all the intra-hour quarters in the corresponding hour  $hr$ .  $z_t^{DA}$  is used to represent all

$$233 \text{ variables in the day-ahead energy schedule, } z_t^{DA} \in \left\{ P_{vpp,t}^{DA}, P_{vpp,t}^{DA+}, P_{vpp,t}^{DA-}, P_{pv,t}^{DA}, P_{chp,t}^{DA}, S_{se,t}^{DA,dch}, S_{se,t}^{DA,ch}, P_{ec,t}^{DA}, \mathcal{G}_{vpp,t}^{DA}, \right. \\ 234 \left. \mathcal{G}_{chp,t}^{DA}, \mathcal{G}_{gb,t}^{DA}, h_{chp,t}^{DA}, h_{gb,t}^{DA}, S_{st,t}^{DA,dch}, S_{st,t}^{DA,ch}, h_{ac,t}^{DA}, c_{ec,t}^{DA}, c_{ac,t}^{DA}, D_{dc,t}^{DA} \right\}.$$

### 235 2.2.3 Constraints of day-ahead reserve schedule

236 From the perspective of MEVPP, upward reserve and downward reserve refer to the ability it can carry upward  
 237 and downward its power output, respectively, without violating corresponding technical constraints. Therefore, in  
 238 Eq.(18) the upward reserve provided by MEVPP is the sum of the technically feasible upward reserves of all  
 239 electricity devices inside MEVPP and the downward reserve in Eq.(19) follows the same rule.

$$\sum_{w \in W_u} A_{vpp,t,w}^{DA,u} = \sum_{pv,chp,se,ec,de \in DV \cup DS \cup DM} (A_{pv,t}^{DA,u} + A_{chp,t}^{DA,u} + A_{se,t}^{DA,u} + A_{ec,t}^{DA,u} + A_{de,t}^{DA,u}) \quad (18)$$

$$\sum_{w \in W_d} A_{vpp,t,w}^{DA,d} = \sum_{pv,chp,se,ec,de \in DV \cup DS \cup DM} (A_{pv,t}^{DA,d} + A_{chp,t}^{DA,d} + A_{se,t}^{DA,d} + A_{ec,t}^{DA,d} + A_{de,t}^{DA,d}) \quad (19)$$

241 MEVPP needs to follow some regulations for the quality of reserve service, such as the minimum offer/bid size  
 242 and the minimum delivery duration. Eq.(20)-(21) define the maximum and minimum offer/bid size of upward and  
 243 downward reserves. Binary variables  $I_{vpp,t,w}^u$  and  $I_{vpp,t,w}^d$  are used to activate/reactivate the strategies in  $W_u$  and  $W_d$ .  
 244 Eq.(22)-(23) force that at maximum one strategy in  $W_u$  or  $W_d$  can be activated. Eq.(24)-(25) find the activation  
 245 time of upward and downward reserve services by binaries  $I_{vpp,t}^{u,su}$  and  $I_{vpp,t}^{d,su}$ , respectively. Eq.(26)-(27) control the  
 246 minimum delivery duration of upward and downward reserves. When the reserve service is activated at time  $t$ , it  
 247 should stay in “on” state for no less than  $|H|$  (the length of set  $H$ ) periods, which for example, should be 120  
 248 minutes for the tertiary spinning reserve [11]. Moreover, the provided reserve should be stable during (at least) the  
 249 minimum delivery duration  $|H|$ , which is controlled by Eq.(28)-(31) under the assumption that the reserve  
 250 schedule in the previous day also follows this regulation. Here,  $M$  is a big enough value. Eq.(28)-(29) can check if  
 251 the reserves offer and bid are stable during the minimum delivery duration  $|H|$ . If they do, auxiliary binary  
 252 variables  $x_{vpp,t}^{u,sta}$  and  $x_{vpp,t}^{d,sta}$  equal to 1, otherwise, they equal to 0. Eq.(30)-(31) control the reserve stability by  $x_{vpp,t}^{u,sta}$   
 253 and  $x_{vpp,t}^{d,sta}$ . Only when the reserve offer/bid has already met the minimum delivery duration  $|H|$  ( $x_{vpp,t}^{u,sta}$  and  $x_{vpp,t}^{d,sta}$   
 254 equal to 1), can MEVPP change the offer/bid quantity, otherwise, it should stay the same as the last time interval.

$$I_{vpp,t,w}^u \cdot \underline{A}_{vpp}^{DA,u} \leq A_{vpp,t,w}^{DA,u} \leq I_{vpp,t,w}^u \cdot \overline{A}_{vpp}^{DA,u} \quad (20)$$

$$I_{vpp,t,w}^d \cdot \underline{A}_{vpp}^{DA,d} \leq A_{vpp,t,w}^{DA,d} \leq I_{vpp,t,w}^d \cdot \overline{A}_{vpp}^{DA,d} \quad (21)$$

$$\sum_{w \in W_u} I_{vpp,t,w}^u \leq 1 \quad (22)$$

$$\sum_{w \in W_d} I_{vpp,t,w}^d \leq 1 \quad (23)$$

$$I_{vpp,t}^{u,su} = \sum_{w \in W_u} (I_{vpp,t,w}^u - I_{vpp,t-1,w}^u) \quad (24)$$

$$I_{vpp,t}^{d,su} = \sum_{w \in W_d} (I_{vpp,t,w}^d - I_{vpp,t-1,w}^d) \quad (25)$$

$$\sum_{w \in W_u} I_{vpp,t+\tau,w}^u \geq I_{vpp,t}^{u,su}, \quad \forall \tau \in H \quad (26)$$

$$\sum_{w \in W_d} I_{vpp,t+\tau,w}^d \geq I_{vpp,t}^{d,su}, \quad \forall \tau \in H \quad (27)$$

$$-(1 - x_{vpp,t}^{u,sta}) \cdot M \leq \sum_{w \in W_u} \left( A_{vpp,t-1,w}^{DA,u} - A_{vpp,t-|H|,w}^{DA,u} \right) \leq (1 - x_{vpp,t}^{u,sta}) \cdot M \quad (28)$$

$$-(1 - x_{vpp,t}^{d,sta}) \cdot M \leq \sum_{w \in W_d} \left( A_{vpp,t-1,w}^{DA,d} - A_{vpp,t-|H|,w}^{DA,d} \right) \leq (1 - x_{vpp,t}^{d,sta}) \cdot M \quad (29)$$

$$-x_{vpp,t}^{u,sta} \cdot M \leq \sum_{w \in W_u} \left( A_{vpp,t,w}^{DA,u} - A_{vpp,t-1,w}^{DA,u} \right) \leq x_{vpp,t}^{u,sta} \cdot M \quad (30)$$

$$-x_{vpp,t}^{d,sta} \cdot M \leq \sum_{w \in W_d} \left( A_{vpp,t,w}^{DA,d} - A_{vpp,t-1,w}^{DA,d} \right) \leq x_{vpp,t}^{d,sta} \cdot M \quad (31)$$

257 MEVPP needs to follow Eq.(32) if participates in CM. Based on the CM contract [34], MEVPP needs to offer on  
 258 DAM and ASM no less than the contracted capacity quantity  $P_{vpp}^{CM}$  during the specified period (usually peak hours)  
 259 represented by specified parameter  $I_{vpp,t}^{CM}$ . During the period when MEVPP needs to follow the contract,  $I_{vpp,t}^{CM}$   
 260 equals to 1; otherwise, it equals to 0.

$$P_{vpp,t}^{DA} + \sum_{w \in W_u} A_{vpp,t,w}^{DA,u} \geq I_{vpp,t}^{CM} \cdot P_{vpp}^{CM} \quad (32)$$

262

#### 263 2.2.4 Constraints of real-time energy schedule

264 When it comes to real-time stage, the day-ahead energy schedule is updated to real-time energy schedule  
 265 according to real-time conditions. Eq.(33)-(36) represent the electricity balance, natural gas balance, heat balance  
 266 and cooling balance of MEVPP, respectively.

267

$$P_{vpp,t}^{RT} = \sum_{\substack{pv,chp,se,ec, \\ de \in DV \cup DS \cup DM}} \left( P_{pv,t}^{RT} + P_{chp,t}^{RT} + (s_{se,t}^{RT,dch} - s_{se,t}^{RT,ch}) - P_{ec,t}^{RT} - D_{de,t}^{RT} \right) \quad (33)$$

$$g_{vpp,t}^{RT} = \sum_{chp,gb \in DV} \left( g_{chp,t}^{RT} + g_{gb,t}^{RT} \right) \quad (34)$$

$$0 = \sum_{\substack{chp,gb,st,ac, \\ dh \in DV \cup DS \cup DM}} \left( -h_{chp,t}^{RT} - h_{gb,t}^{RT} - (s_{st,t}^{RT,dch} - s_{st,t}^{RT,ch}) + h_{ac,t}^{RT} + D_{dh,t}^{DA} \right) \quad (35)$$

$$0 = \sum_{ec,ac,dc \in DV \cup DM} \left( -c_{ec,t}^{RT} - c_{ac,t}^{RT} + D_{dc,t}^{RT} \right) \quad (36)$$

268

269 Eq.(37) calculates the deviation between real-time energy schedule and day-ahead energy schedule caused by  
 270 uncertainties. Eq.(38) forces the imbalance of both withdrawal and injection directions to be non-negative. They are  
 271 made complementary by the imbalance cost minimization term in the objective function.

272

$$P_{vpp,t}^{EIP+} - P_{vpp,t}^{EIP-} = P_{vpp,t}^{RT} - P_{vpp,t}^{DA} \quad (37)$$

$$P_{vpp,t}^{EIP+} \cdot P_{vpp,t}^{EIP-} \geq 0 \quad (38)$$

273

#### 274 2.2.5 Constraints of real-time reserve schedule

275 After the real-time energy schedule, the real-time reserve schedule is calculated by Eq.(39)-(40). The total  
 276 reserve MEVPP can provide is limited by the reserve each device can technically provide in real-time stage.

277

$$A_{vpp,t}^{RT,u} = \sum_{\substack{pv,chp,se,ec, \\ de \in DV \cup DS \cup DM}} \left( A_{pv,t}^{RT,u} + A_{chp,t}^{RT,u} + A_{se,t}^{RT,u} + A_{ec,t}^{RT,u} + A_{de,t}^{RT,u} \right) \quad (39)$$

$$A_{vpp,t}^{RT,d} = \sum_{\substack{pv,chp,se,ec, \\ de \in DV \cup DS \cup DM}} \left( A_{pv,t}^{RT,d} + A_{chp,t}^{RT,d} + A_{se,t}^{RT,d} + A_{ec,t}^{RT,d} + A_{de,t}^{RT,d} \right) \quad (40)$$

278 The unsupplied reserve is the difference between the reserve requirement from TSO and the real-time reserve  
 279 schedule of MEVPP. The calculation of unsupplied reserve follows the rules of Terna (Italian TSO) [9]. Taking  
 280 upward reserve as an example, if upward reserve is requested then the network is imbalanced in the direction of  
 281 lack of generation. If in real-time energy schedule (real-time baseline) MEVPP produces electricity no less than in  
 282 day-ahead energy schedule (day-ahead baseline), then MEVPP presents an excess of generation, so it positively

283 compensates the network imbalance. In this case, MEVPP only needs to provide upward reserve no less than its  
 284 accepted offer in ASM. However, if in real-time energy schedule MEVPP produces less than in day-ahead energy  
 285 schedule, then it contributes to the power imbalance of the network. In this case, MEVPP needs to supply upward  
 286 reserve firstly to make up its power imbalance, and then to realize its accepted offer in ASM. Otherwise, it will be  
 287 penalized. The downward reserve follows the same rule but in the opposite direction. Eq.(41)-(42) calculate the  
 288 unsupplied reserve following the above rules for both upward and downward directions, respectively. Terms  
 289  $(1 - \sum_{w \in W_u} I_{vpp,t,w}^u) \cdot M$  and  $(1 - \sum_{w \in W_d} I_{vpp,t,w}^d) \cdot M$  use a big enough value  $M$  to ensure that when MEVPP does not  
 290 participate in ASM, it can be neglected from the URP. Eq.(43) sets the unsupplied reserves to be non-negative.

$$A_{vpp,t}^{RT,u} + P_{vpp,t}^{URP,u} \geq \max \left\{ P_{vpp,t}^{DA} - P_{vpp,t}^{RT} - (1 - \sum_{w \in W_u} I_{vpp,t,w}^u) \cdot M, 0 \right\} + \sum_{w \in W_u} A_{vpp,t,w}^{DA,u} \quad (41)$$

$$A_{vpp,t}^{RT,d} + P_{vpp,t}^{URP,d} \geq \max \left\{ P_{vpp,t}^{RT} - P_{vpp,t}^{DA} - (1 - \sum_{w \in W_d} I_{vpp,t,w}^d) \cdot M, 0 \right\} + \sum_{w \in W_d} A_{vpp,t,w}^{DA,d} \quad (42)$$

$$P_{vpp,t}^{URP,u}, P_{vpp,t}^{URP,d} \geq 0 \quad (43)$$

291

## 292 2.2.6 Constraints of final dispatching

293 To calculate the operational cost of all the devices and the final natural gas consumption cost, MEVPP needs to  
 294 consider its final dispatching after the reserve deployment by TSO. In Eq.(44), according to the price strategy  
 295 MEVPP chose in ASM, there exists  $\sigma_{t,w}^{ASM,u}$  probability that the upward reserve is accepted and  $(1 - \sigma_{t,w}^{ASM,u})$   
 296 probability that the upward reserve is rejected. Therefore, the final dispatching after upward reserve deployment is  
 297 calculated by Eq.(44). Eq.(45) which is for downward reserve deployment follows the same rule as Eq.(44).  
 298

$$P_{vpp,t}^{f,u} = \sum_{w \in W_u} \left[ \sigma_{t,w}^{ASM,u} \cdot (P_{vpp,t}^{RT} + A_{vpp,t,w}^{RT,u}) + (1 - \sigma_{t,w}^{ASM,u}) \cdot P_{vpp,t}^{RT} \right] \quad (44)$$

$$P_{vpp,t}^{f,d} = \sum_{w \in W_d} \left[ \sigma_{t,w}^{ASM,d} \cdot (P_{vpp,t}^{RT} - A_{vpp,t,w}^{RT,d}) + (1 - \sigma_{t,w}^{ASM,d}) \cdot P_{vpp,t}^{RT} \right] \quad (45)$$

299 Power constraints in the final dispatching after upward reserve deployment and downward reserve deployment  
 300 follow the same rules as the real-time energy schedule in Eq.(33)-(36), which are not repeated here. However, the

301 variables are now changed to  $z_t^{f,u} \in \left\{ P_{vpp,t}^{f,u}, P_{pv,t}^{f,u}, P_{chp,t}^{f,u}, S_{se,t}^{f,u,dch}, S_{se,t}^{f,u,ch}, P_{ec,t}^{f,u}, D_{de,t}^{f,u}, G_{vpp,t}^{f,u}, G_{chp,t}^{f,u} \right\}$  and

302  $z_t^{f,d} \in \left\{ P_{vpp,t}^{f,d}, P_{pv,t}^{f,d}, P_{chp,t}^{f,d}, S_{se,t}^{f,d,dch}, S_{se,t}^{f,d,ch}, P_{ec,t}^{f,d}, D_{de,t}^{f,d}, G_{vpp,t}^{f,d}, G_{chp,t}^{f,d}, G_{gb,t}^{f,d}, h_{chp,t}^{f,d}, h_{gb,t}^{f,d}, S_{st,t}^{f,d,dch}, S_{st,t}^{f,d,ch}, h_{ac,t}^{f,d}, c_{ec,t}^{f,d}, c_{ac,t}^{f,d}, D_{dc,t}^{f,d} \right\}$ , respectively.

303 Eq.(46)-(47) calculate the natural gas deviation between final dispatching and day-ahead energy schedule, which  
 304 are represented by  $\Delta g_{vpp,t}^{f,u}$  and  $\Delta g_{vpp,t}^{f,d}$ . The proportions of upward reserve request and downward reserve request  
 305 from TSO are considered in Eq.(48). The deviation is separated into injection and withdrawal directions in Eq.(48),  
 306 both of which are non-negative limited by Eq.(49).  
 307

$$\Delta g_{vpp,t}^{f,u} = g_{vpp,t}^{f,u} - g_{vpp,t}^{DA} \quad (46)$$

$$\Delta g_{vpp,t}^{f,d} = g_{vpp,t}^{f,d} - g_{vpp,t}^{DA} \quad (47)$$

$$g_{vpp,t}^{GIP+} - g_{vpp,t}^{GIP-} = \chi_t^u \cdot \Delta g_{vpp,t}^{f,u} + \chi_t^d \cdot \Delta g_{vpp,t}^{f,d} \quad (48)$$

$$g_{vpp,t}^{GIP+}, g_{vpp,t}^{GIP-} \geq 0 \quad (49)$$

## 308 2.3. MEVPP structure

309 The general structure of MEVPP is given in the physical layer in Fig.1. It aggregates PV generators, CHPs, gas  
 310 boilers (GBs), electric chillers (ECs), absorption chillers (ACs), electrical energy storages (SEs), thermal energy  
 311 storages (STs), flexible electrical demands (DEs) and TCLs. For simplification, in the following constraints, index  
 312  $S1 \in T_{DA} \cup T_{RT} \cup T_{final}$  in the superscript is used when the formula is valid in day-ahead schedule, real-time schedule

313 and final dispatching. Index  $S2 \in T_{DA} \cup T_{RT}$  in the superscript is used when the formula is valid in day-ahead  
 314 schedule and real-time schedule. Index  $S3 \in T_{RT} \cup T_{final}$  in the superscript is used when the formula is valid in real-  
 315 time schedule and final dispatching.  
 316

### 317 2.3.1 Energy constraints of energy conversion devices and storages

318 The energy conversion efficiencies of CHP, GB, EC and AC are given in Eq.(50) [25]. Their operational upper  
 319 and lower bounds are limited by Eq.(51)-(53). Binary variable  $I_{chp,t}^{DA}$  is used for the on/off state of CHP in (51),  
 320 which is determined in day-ahead schedule. Eq.(52) computes the start-up and shut-down states of CHP. CHP also  
 321 needs to follow ramping limits in Eq.(54)-(55). Eq.(56)-(57) limit charging and discharging powers of SE and ST.  
 322 Subscript  $k \in DS$  is used to represent both SE and ST. An auxiliary binary variable  $x_{k,t}^{S1}$  is introduced to  
 323 characterize the complementarity between charging and discharging states. Eq.(58) presents the electrical and heat  
 324 energy stored in SE and ST at the end of each time interval  $\Delta t$ . Eq.(59) imposes the limitation of SOC. At the end  
 325 of the day, the SOCs of SE and ST need to go back to the initial  $SOC_{k,INI}^{S1}$  for the new operational cycle in the  
 326 following day, this is modeled in Eq.(60). Eq.(61) limits the battery cycles per day for SE, to avoid the maximum  
 327 number of cycles  $lfcl$  occur before the expected lifetime year  $lfyr$ . The 4 in the denominator is for time unit  
 328 consistency.

$$\begin{cases} P_{chp,t}^{S1} = \eta_{chp}^e \cdot G_{chp,t}^{S1} \\ h_{chp,t}^{S1} = \left[ (1 - \eta_{chp}^e - \eta_{chp}^{loss}) \cdot \eta_{chp}^{hrs} \right] / \eta_{chp}^e \cdot P_{chp,t}^{S1} \\ h_{gb,t}^{S1} = \eta_{gb} \cdot G_{gb,t}^{S1} \\ c_{ec,t}^{S1} = COP_{ec} \cdot P_{ec,t}^{S1} \\ c_{ac,t}^{S1} = COP_{ac} \cdot h_{ac,t}^{S1} \end{cases} \quad (50)$$

$$I_{chp,t}^{DA} \cdot \underline{P}_{chp} \leq P_{chp,t}^{S1} \leq I_{chp,t}^{DA} \cdot \overline{P}_{chp} \quad (51)$$

$$I_{chp,t}^{DA,su} - I_{chp,t}^{DA,sd} = I_{chp,t}^{DA} - I_{chp,t-1}^{DA} \quad (52)$$

$$\begin{cases} 0 \leq h_{gb,t}^{S1} \leq \overline{H}_{gb} \\ 0 \leq c_{ec,t}^{S1} \leq \overline{C}_{ec} \\ 0 \leq c_{ac,t}^{S1} \leq \overline{C}_{ac} \end{cases} \quad (53)$$

$$P_{chp,t}^{S1} - P_{chp,t-1}^{S1} \leq (1 - I_{chp,t}^{DA,su}) \cdot R_{chp}^u + I_{chp,t}^{DA,su} \cdot \underline{P}_{chp} \quad (54)$$

$$P_{chp,t}^{S1} - P_{chp,t-1}^{S1} \geq -(1 - I_{chp,t}^{DA,sd}) \cdot R_{chp}^d - I_{chp,t}^{DA,sd} \cdot \underline{P}_{chp} \quad (55)$$

$$x_{k,t}^{S1} \cdot \underline{S}_{k,t}^{ch} \leq s_{k,t}^{S1,ch} \leq x_{k,t}^{S1} \cdot \overline{S}_{k,t}^{ch}, \forall k \in DS \quad (56)$$

$$(1 - x_{k,t}^{S1}) \cdot \underline{S}_{k,t}^{dch} \leq s_{k,t}^{S1,dch} \leq (1 - x_{k,t}^{S1}) \cdot \overline{S}_{k,t}^{dch}, \forall k \in DS \quad (57)$$

$$E_{k,t}^{S1} = E_{k,t-1}^{S1} + (s_{k,t}^{S1,ch} \cdot \eta_k^{ch} - s_{k,t}^{S1,dch} / \eta_k^{dch}) \cdot \Delta t, \forall k \in DS \quad (58)$$

$$\underline{SOC}_k \leq E_{k,t}^{S1} / CAP_k \leq \overline{SOC}_k, \forall k \in DS \quad (59)$$

$$SOC_{k,Nt}^{S1} = SOC_{k,INI}^{S1}, \forall k \in DS \quad (60)$$

$$\frac{\sum_t s_{se,t}^{S1,dch}}{4 \cdot CAP_{se} \cdot (\overline{SOC}_{se} - \underline{SOC}_{se})} \leq \frac{lfcl}{lfyr \cdot 365} \quad (61)$$

330

### 331 2.3.2 Energy constraints of PV output

332 Eq.(62) sets the upper and lower bounds of PV output on day D-1. The upper bound is the day-ahead available

333 PV capacity, defined as the maximum power PV can produce at estimated solar radiation. On day D, the upper  
 334 bound of PV output is the real-time available PV capacity given in (64) which is an uncertain parameter affected by  
 335 weather forecast errors.

$$0 \leq p_{pv,t}^{DA} \leq P_{pv,t}^{DA,a} \quad (62)$$

$$p_{pv,t}^{S3} \geq 0 \quad (63)$$

$$p_{pv,t}^{S3} \leq \bar{P}_{pv,t}^{RT,a} \quad (64)$$

336 RO model is formed to represent the uncertain real-time available PV capacity as follows:

$$337 \quad \tilde{P}_{pv,t}^{RT,a} = P_{pv,t}^{RT,a} + \gamma_{pv,t}^{RT} \cdot \bar{P}_{pv,t}^{RT,a}$$

338 where

$$339 \quad P_{pv,t}^{RT,a} = \frac{1}{2} \left( \overline{P_{pv,t}^{RT,a}} + \underline{P_{pv,t}^{RT,a}} \right), \bar{P}_{pv,t}^{RT,a} = \frac{1}{2} \left( \overline{P_{pv,t}^{RT,a}} - \underline{P_{pv,t}^{RT,a}} \right).$$

340 The uncertain parameter  $\bar{P}_{pv,t}^{RT,a}$  fluctuates within the interval under a certain confidence level. Parameter  $P_{pv,t}^{RT,a}$  is  
 341 the deterministic term which equals to  $P_{pv,t}^{DA,a}$ . Parameter  $\bar{P}_{pv,t}^{RT,a}$  defines the fluctuation interval, which is the  
 342 maximum deviation of the parameter. Parameters  $\overline{P_{pv,t}^{RT,a}}$  and  $\underline{P_{pv,t}^{RT,a}}$  are the upper and lower bounds of real-time  
 343 available PV capacity. Variable  $\gamma_{pv,t}^{RT}$  defines the confidence level, ranging within [-1,1]. The budget of uncertainty  
 344  $\Gamma_{pv,t}^{RT}$  is introduced to control the robustness level against PV output deviation. Since there is only one uncertain  
 345 parameter  $\bar{P}_{pv,t}^{RT,a}$  in (64) for a PV generator at each time  $t$ ,  $\Gamma_{pv,t}^{RT}$  ranges within [0,1]. The robust counterpart of  
 346 Eq.(64) is formulated as [31]:

$$p_{pv,t}^{S3} + \max \gamma_{pv,t}^{RT} \cdot \bar{P}_{pv,t}^{RT,a} \cdot \left| \rho_{pv,t}^{S3} \right| \leq P_{pv,t}^{RT,a}$$

$$0 \leq \gamma_{pv,t}^{RT} \leq 1, v_{pv,t}^{S3}$$

$$348 \quad \gamma_{pv,t}^{RT} \leq \Gamma_{pv,t}^{RT}, \alpha_{pv,t}^{S3}$$

349 where  $v_{pv,t}^{S3}, \alpha_{pv,t}^{S3}$  are dual variables of the corresponding constraints.  $\rho_{pv,t}^{S3}$  is an auxiliary variable to build a standard  
 350 robust model and is forced to be equal to 1. After using the absolute function  $\left| \rho_{pv,t}^{S3} \right|$ , variable  $\gamma_{pv,t}^{RT}$  ranges within  
 351 [0,1]. The maximum problem formulated can be equally converted to the dual minimization problem through the  
 352 strong duality theory as follows:

$$\begin{cases} p_{pv,t}^{S3} + \alpha_{pv,t}^{S3} \cdot \Gamma_{pv,t}^{RT} + v_{pv,t}^{S3} \leq P_{pv,t}^{RT,a} \\ \alpha_{pv,t}^{S3} + v_{pv,t}^{S3} \geq \bar{P}_{pv,t}^{RT,a} \cdot \gamma_{pv,t}^{S3} \\ \alpha_{pv,t}^{S3} \geq 0 \\ v_{pv,t}^{S3} \geq 0 \\ \gamma_{pv,t}^{S3} \geq 1 \end{cases} \quad (65)$$

353 where  $\gamma_{pv,t}^{S3}$  is used to linearize the absolute function  $\left| \rho_{pv,t}^{S3} \right|$ . Constraint (64) is finally converted to Eq.(65).

354

### 355 2.3.3 Energy constraints of flexible demands

356 Eq.(66) limits DE after considering the demand management on day D. For the computation of demand  
 357 management cost in Eq.(8), DE in the final dispatching is calculated by Eq.(67) when upward reserve is deployed,  
 358 or by Eq.(68) when downward reserve is deployed. Eq.(69)-(72) limit the demand management of both directions.  
 359 Auxiliary binary variables  $x_{de,t}^{fu}$  and  $x_{de,t}^{fid}$  are used to guarantee that DE cannot curtail and increase simultaneously.

360

$$D_{de,t}^{DA} - D_{de,t}^m \leq D_{de,t}^{S3} \leq D_{de,t}^{DA} + D_{de,t}^p \quad (66)$$

$$D_{de,t}^{fu} = D_{de,t}^{DA} - d_{de,t}^{fu,m} + d_{de,t}^{fu,p} \quad (67)$$

$$D_{de,t}^{fid} = D_{de,t}^{DA} - d_{de,t}^{fid,m} + d_{de,t}^{fid,p} \quad (68)$$

$$0 \leq d_{de,t}^{f^{iu},m} \leq (1 - x_{de,t}^{f^{iu}}) \cdot \overline{D_{de,t}^m} \quad (69)$$

$$0 \leq d_{de,t}^{f^{iu},p} \leq x_{de,t}^{f^{iu}} \cdot \overline{D_{de,t}^p} \quad (70)$$

$$0 \leq d_{de,t}^{f^{id},m} \leq (1 - x_{de,t}^{f^{id}}) \cdot \overline{D_{de,t}^m} \quad (71)$$

$$0 \leq d_{de,t}^{f^{id},p} \leq x_{de,t}^{f^{id}} \cdot \overline{D_{de,t}^p} \quad (72)$$

361

362

363

364

365

366

367

368

The flexible cooling demand is a kind of TCL. Eq.(73) defines the temporal trajectories of indoor temperature for TCLs [41]. Parameter  $\alpha_{dc}$  is defined as  $\alpha_{dc} = e^{-\Delta t / (C_{dc} \cdot R_{dc})}$ ;  $\Delta t$  is the size of the time interval;  $R_{dc}$  and  $C_{dc}$  are the thermal resistance and thermal capacitance. Parameter  $\theta_t^o$  is the outdoor temperature. Eq.(74) sets the on/off condition of cooling devices by a binary variable  $I_{dc,t}^{S1}$ . The cooling devices are turned on only when the indoor temperatures of TCLs exceed their satisfactory temperatures  $\theta_{dc,t}^{S1,sa}$ . Considering consumers' insensitive feeling within a certain range of indoor temperature, Eq.(75) defines the acceptable temperature range of TCL.

$$\theta_{dc,t}^{S1} = \alpha_{dc} \cdot \theta_{dc,t-1}^{S1} + (1 - \alpha_{dc}) \cdot (\theta_t^o - I_{dc,t}^{S1} \cdot R_{dc} \cdot D_{dc,t}^{S1}) \quad (73)$$

$$I_{dc,t}^{S1} = \begin{cases} 1, & \theta_{dc,t}^{S1} \geq \theta_{dc,t}^{S1,sa} \\ 0, & \theta_{dc,t}^{S1} \leq \theta_{dc,t}^{S1,sa} \end{cases} \quad (74)$$

$$\underline{\theta_{dc}^{S1}} \leq \theta_{dc,t}^{S1} \leq \overline{\theta_{dc}^{S1}} \quad (75)$$

369

370

#### 2.3.4 Reserve constraints

371

372

373

374

375

376

The electricity devices can provide reserves according to their technical capacity margins. Eq.(76)-(77) limit the upward and downward reserves provided by CHP. Eq.(78)-(79) are the ramping limits of CHP. Eq.(80)-(81) limit the upward and downward reserves provided by EC. As a kind of electricity-consuming device, the upward (downward) reserve of EC represents its ability to carry downward (upward) its power output. Eq.(82) limits the downward reserve and Eq.(83)-(85) limit the upward reserve provided by PV in day-ahead schedule and real-time schedule.

$$0 \leq A_{chp,t}^{S2,u} \leq I_{chp,t}^{DA} \cdot \overline{P_{chp}} - p_{chp,t}^{S2} \quad (76)$$

$$0 \leq A_{chp,t}^{S2,d} \leq p_{chp,t}^{S2} - I_{chp,t}^{DA} \cdot \underline{P_{chp}} \quad (77)$$

$$(p_{chp,t}^{S2} + A_{chp,t}^{S2,u}) - (p_{chp,t-1}^{S2} - A_{chp,t-1}^{S2,d}) \leq (1 - I_{chp,t}^{DA, su}) \cdot R_{chp}^u + I_{chp,t}^{DA, su} \cdot \underline{P_{chp}} \quad (78)$$

$$(p_{chp,t}^{S2} - A_{chp,t}^{S2,d}) - (p_{chp,t-1}^{S2} + A_{chp,t-1}^{S2,u}) \geq -(1 - I_{chp,t}^{DA, sd}) \cdot R_{chp}^d - I_{chp,t}^{DA, sd} \cdot \underline{P_{chp}} \quad (79)$$

$$0 \leq A_{ec,t}^{S2,u} \leq p_{ec,t}^{S2} - \underline{P_{ec}} \quad (80)$$

$$0 \leq A_{ec,t}^{S2,d} \leq \overline{P_{ec}} - p_{ec,t}^{S2} \quad (81)$$

$$0 \leq A_{pv,t}^{S2,d} \leq p_{pv,t}^{S2} \quad (82)$$

$$0 \leq A_{pv,t}^{DA,u} \leq \overline{P_{pv,t}^{DA,a}} - p_{pv,t}^{DA} \quad (83)$$

$$A_{pv,t}^{RT,u} \geq 0 \quad (84)$$

$$A_{pv,t}^{RT,u} \leq \overline{P_{pv,t}^{RT,a}} - p_{pv,t}^{RT} \quad (85)$$

377

378

The method to deal with the uncertainty of real-time available PV capacity  $\overline{P_{pv,t}^{RT,a}}$  in Eq.(85) is the same approach as used by Eq.(64). RO model is formed and Eq.(85) is finally converted to Eq.(86):

$$\begin{cases} A_{pv,t}^{RT,u} + \alpha_{pv,t}^{RT,u} \cdot \Gamma_{pv,t}^{RT} + v_{pv,t}^{RT,u} \leq P_{pv,t}^{RT,a} - p_{pv,t}^{RT} \\ \alpha_{pv,t}^{RT,u} + v_{pv,t}^{RT,u} \geq \bar{P}_{pv,t}^{RT,a} \cdot y_{pv,t}^{RT,u} \\ \alpha_{pv,t}^{RT,u} \geq 0 \\ v_{pv,t}^{RT,u} \geq 0 \\ y_{pv,t}^{RT,u} \geq 1 \end{cases} \quad (86)$$

379 It is the same as in Eq.(65) that,  $v_{pv,t}^{RT,u}, \alpha_{pv,t}^{RT,u}$  are dual variables of the robust counterpart.  $y_{pv,t}^{RT,u}$  is an auxiliary  
380 variable for linearization.

381 For the electricity demands, the upward and downward reserves in day-ahead and real-time schedules are limited  
382 by their demand management abilities, as in Eq.(87)-(88).

$$0 \leq A_{de,t}^{S2,u} \leq D_{de,t}^{S2} - \left( D_{de,t}^{DA} - \overline{D_{de,t}^m} \right) \quad (87)$$

$$0 \leq A_{de,t}^{S2,d} \leq \left( D_{de,t}^{DA} + \overline{D_{de,t}^p} \right) - D_{de,t}^{S2} \quad (88)$$

383 Eq.(89)-(90) set the upward and downward reserves of SE considering discharging and charging power limits.  
384 For SE, not only the power constraints but also the SOC constraints need to be considered. Eq.(91)-(92) compute  
385 the electrical energy stored in SE at the end of each time interval considering the upward reserve and downward  
386 reserve qualities SE can provide. The limitations of SOC are in Eq.(93)-(94). Theoretically, at the end of the day,  
387 the SOC of SE needs to go back to the initial state (or close to the initial state) to start a new round of work on the  
388 following day. Because SE is normally a short-term intraday energy storage. Therefore, to ensure that the reserve  
389 band provided by SE can always be deployed without affecting its new round of work on the following day, Eq.(95)  
390 guarantees that the upward and downward reserves provided by the SE cannot be activated simultaneously and  
391 Eq.(96) forces the sum of upward and downward reserves provided throughout a day to be equal, considering the  
392 discharging and charging efficiencies.

$$0 \leq A_{se,t}^{S2,u} \leq \overline{S_{se}^{dch}} - S_{se,t}^{S2,dch} + S_{se,t}^{S2,ch} \quad (89)$$

$$0 \leq A_{se,t}^{S2,d} \leq \overline{S_{se}^{ch}} + S_{se,t}^{S2,dch} - S_{se,t}^{S2,ch} \quad (90)$$

$$E_{se,t}^{S2,AS,u} = E_{se,t-1}^{S2,AS,u} + E_{se,t}^{S2} - E_{se,t-1}^{S2} - \left( A_{se,t}^{S2,u} / \eta_{se}^{dch} \right) \cdot \Delta t \quad (91)$$

$$E_{se,t}^{S2,AS,d} = E_{se,t-1}^{S2,AS,d} + E_{se,t}^{S2} - E_{se,t-1}^{S2} + A_{se,t}^{S2,d} \cdot \eta_{se}^{ch} \cdot \Delta t \quad (92)$$

$$\overline{SOC_{se}} \leq E_{se,t}^{S2,AS,u} / CAP_{se} \leq \overline{SOC_{se}} \quad (93)$$

$$\overline{SOC_{se}} \leq E_{se,t}^{S2,AS,d} / CAP_{se} \leq \overline{SOC_{se}} \quad (94)$$

$$A_{se,t}^{S2,u} \cdot A_{se,t}^{S2,d} = 0 \quad (95)$$

$$\sum_t A_{se,t}^{S2,u} / \eta_{se}^{dch} \cdot \Delta t = \sum_t A_{se,t}^{S2,d} \cdot \eta_{se}^{ch} \cdot \Delta t \quad (96)$$

## 394 2.4. Linearization

395 A few of constraints are non-linear in the proposed optimization model, including the maximum functions  
396 inserted in Eq.(41)-(42), the multiplier of a binary variable and a continuous variable in Eq.(73)-(74) and the  
397 incompatibility of two variables in Eq.(95). To improve the accuracy of results and the speed of simulation, these  
398 constraints are linearized in Appendix A and the optimization problem becomes a MILP which can be solved by  
399 GUROBI.

## 400 3. Case study

### 401 3.1. Basic Data

402 The MEVPP consists of a PV generator, a CHP, a GB, an EC, an AC, a SE and a ST. There are a flexible DE, a  
403 fixed heat demand (DH) and a TCL, representing the total demand of MEVPP. A typical day in the summer of 2021  
404 in North Italy is considered. The main input data are briefly provided due to the word limitation. For a detailed  
405 introduction of all input data, please refer to the **SUPPLEMENTARY MATERIAL**.

406 The market data are collected from GME (the Italian power exchange) [38], including DAM prices with hourly  
 407 intervals and ASM prices with 15-minute intervals. The electricity buying price  $\lambda_t^{DAM-}$  is given in Fig.2. The  
 408 electricity selling price  $\lambda_t^{DAM+}$  is set as  $0.5 \cdot \lambda_t^{DAM-}$ . Five levels of  $\sigma_{t,w}^{ASM,u}$ ,  $w = 1 \dots 5$  ( $\sigma_{t,w}^{ASM,d}$ ,  $w = 1 \dots 5$ ) are fixed as 100%,  
 409 100%~80%, 80%~60%, 60%~40% and 40%~20% for all quarters throughout the day, as in Fig.3(a) (Fig.4(a)). For  
 410 each quarter, the offer (bid) prices  $\lambda_{t,w}^{ASM,u}$ ,  $w = 1 \dots 5$  ( $\lambda_{t,w}^{ASM,d}$ ,  $w = 1 \dots 5$ ) are presented in Fig.3(b) (Fig.4(b)). The request  
 411 proportions of upward reserve  $\chi_t^u$  and downward reserve  $\chi_t^d$  throughout the day are presented in Fig.5 [38].

412  
413

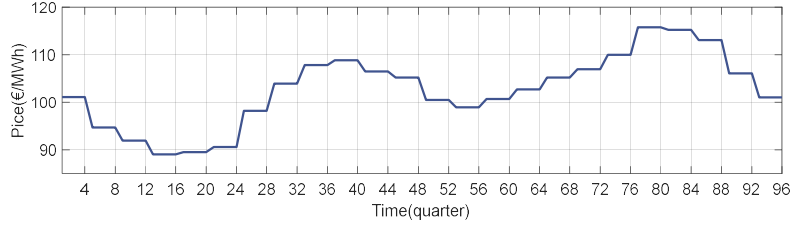
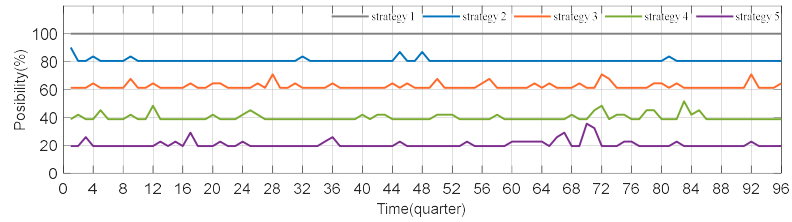


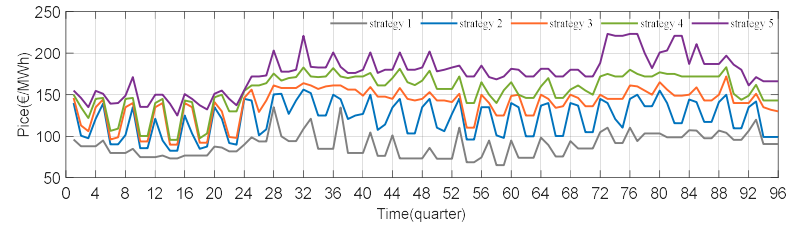
Fig.2 Electricity buying price in DAM,  $\lambda_t^{DAM-}$

414  
415



(a) Probabilities of upward reserve strategies being accepted,  $\sigma_{t,w}^{ASM,u}$

416  
417

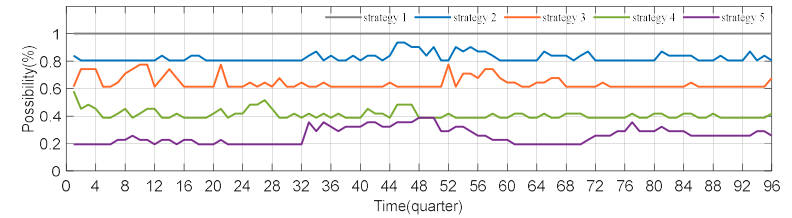


(b) Offer prices of upward reserve strategies,  $\lambda_{t,w}^{ASM,u}$

418

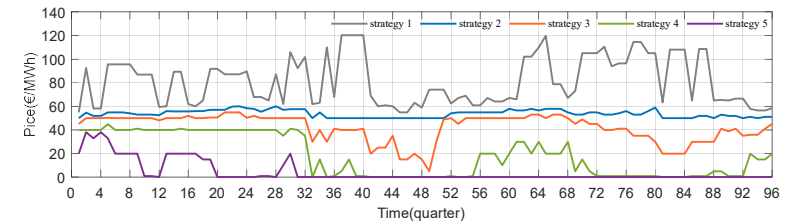
Fig.3 Strategies of upward reserve offers

419  
420



(a) Probabilities of downward reserve strategies being accepted,  $\sigma_{t,w}^{ASM,d}$

421  
422



(b) Bid prices of downward reserve strategies,  $\lambda_{t,w}^{ASM,d}$

423

Fig.4 Strategies of downward reserve bids

424  
425  
426

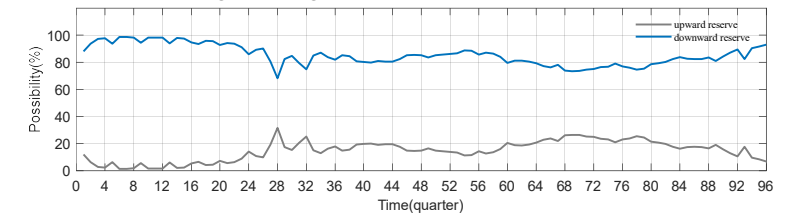
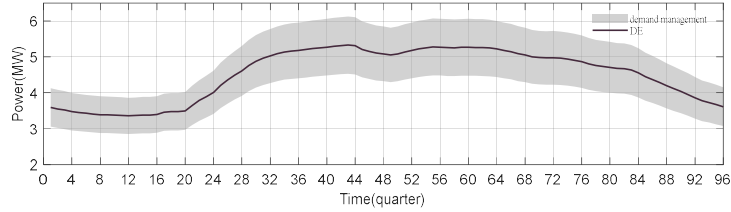
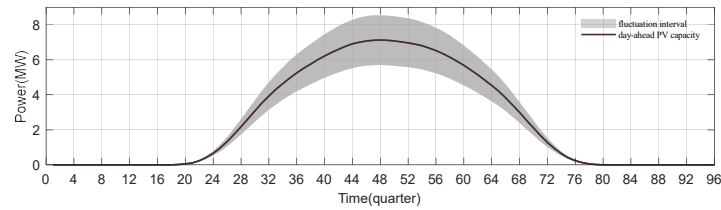


Fig.5 Proportions of upward and downward reserve requests,  $\chi_t^u$  and  $\chi_t^d$

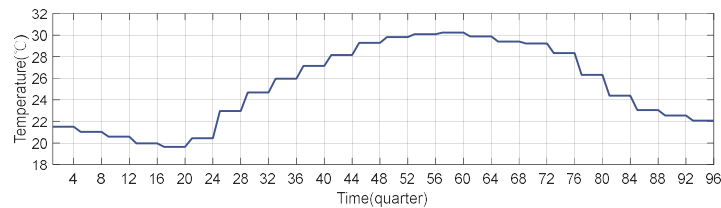
427 The DE value  $D_{de,t}^{DA}$  and PV capacity  $P_{pv,t}^{DA,a}$  are from Terna (the Italian TSO) [39] and are scaled according to the  
 428 requirement of this paper, as in Fig.6 and Fig.7, respectively. The weather temperature  $\theta_t^o$  in Fig.8 is collected from  
 429 Lambrate, Milan, Italy [40]. The minimum delivery duration  $|H|$  is 120 minutes, and the minimum offer/bid size  
 430  $A_{vpp}^{DA,u/d}$  is 1MW [8,9,11]. The values of other parameters are given in Tab.S1 in **SUPPLEMENTARY MATERIAL**  
 431 [39,41].



432 Fig.6 DE value and DE management ability,  $D_{de,t}^{DA}$ ,  $\overline{D_{de,t}^p}$  and  $\overline{D_{de,t}^m}$



433 Fig.7 Available PV capacity and fluctuation interval of PV capacity,  $P_{pv,t}^{DA,a}$  and  $\overline{P_{pv,t}^{RT,a}}$



434 Fig.8 Weather temperature,  $\theta_t^o$

435 The cases for analysis are given in Tab.1. In case 3 scenario *b*, *c*, *d* and *e*, input data need to change following the  
 436 scenario descriptions for analysis.

437 Tab.1 Description of cases

Case	Scenario	DAM	ASM	CM	Uncertainty	Scenario description
1	-	✓	✗	✗	✗	
2	-	✓	✗	✗	✓	
3	<i>a</i>	✓	✓	✗	✓	Reference scenario
	<i>b</i>	✓	✓	✗	✓	Compared to scenario <i>a</i> , proportion of upward reserve request and proportion of downward reserve request from TSO are exchanged
	<i>c</i>	✓	✓	✗	✓	Compared to scenario <i>a</i> , non-electricity devices are not available in reserve deployment
	<i>d</i>	✓	✓	✗	✓	Compared to scenario <i>a</i> , reserve regulation of minimum offer/bid size increases or decreases
	<i>e</i>	✓	✓	✗	✓	Compared to scenario <i>a</i> , reserve regulation of minimum delivery duration increases or decreases
4		✓	✓	✓	✓	

## 442 3.2. Results and discussion

### 443 3.2.1 Case 1 and case 2: Impacts of available PV capacity uncertainty

444 In case 1 and case 2 MEVPP does not participate in ASM and CM. However, in case 2, MEVPP considers the  
 445 uncertainty of available PV capacity. The budget of uncertainty  $\Gamma_{pv,t}^{RT}$  is used to control the robustness level against  
 446 the uncertainty. As can be observed in Fig.9, when the budget of uncertainty increases, the total cost of MEVPP  
 447 goes up. Because MEVPP needs to deal with larger power deviation caused by PV output uncertainty, which  
 448 prevents it from achieving the optimal strategy. But a higher budget of uncertainty comes with a conservative cost  
 449 with less economic risk. In the following analysis,  $\Gamma_{pv,t}^{RT}$  is fixed as 100% in case 2 - case 4 for minimum cost risk.

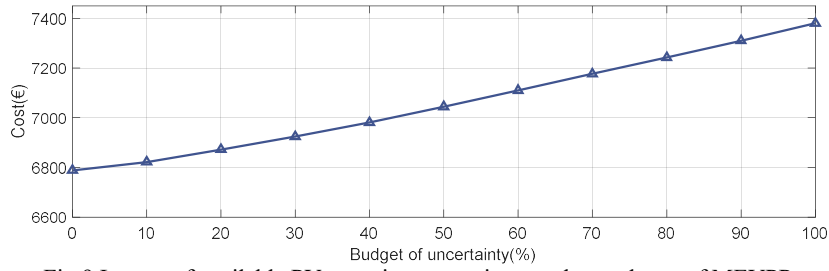


Fig.9 Impact of available PV capacity uncertainty on the total cost of MEVPP

450  
451  
452

453 3.2.2 Case 2 and case 3.a: Impacts of ASM participation

454 In case 3, MEVPP further participates in ASM compared to case 2. Case 3.a (case 3 scenario a) represents the  
455 reference scenario for case 3, in which all the input data are set as the data given in section 3.1.

456 The day-ahead energy and reserve schedules of MEVPP in case 3.a are presented in Fig.10. The specific reserve  
457 schedules of the devices inside MEVPP are also given in Fig.10. During 2:15a.m.-24:00a.m.(quarter 9-96), the day-  
458 ahead energy schedule of case 3.a is higher than case 2, because MEVPP enlarges its power output to provide more  
459 downward reserve, which is profitable for itself. The costs of MEVPP in case 2 and case 3.a are given in Tab.2.  
460 Profits are presented as negative costs.

461 The total cost of MEVPP decreases by 17% from 7379.933€ in case 2 to 6122.362€ in case 3.a, which shows the  
462 profit from reserve transactions in ASM. MEVPP increases its power output in day-ahead energy schedule to  
463 provide more downward reserve as in Fig.10, therefore, the cost of buying energy from DAM decreases from  
464 3428.870€ to 1994.153€. The cost of buying natural gas from GM increases from 2904.966€ to 3595.855€ to  
465 support the power output increasing in day-ahead energy schedule. The electricity imbalance cost in case 2 is  
466 negative because the real-time energy schedule deviates from the day-ahead energy schedule in the withdrawn  
467 direction. The natural gas imbalance costs are negative in both case 2 and case 3.a, which are due to the similar  
468 reason. Moreover, the difference of natural gas imbalance cost between case 2 and case 3.a is high, because in case  
469 3.a the natural gas also needs to support the reserve deployment in the real-time stage compared to case 2.

470 It can also be observed from Fig.10 that, MEVPP provides larger quantity of downward reserve than upward  
471 reserve. Because in the input data (Fig.5 in section 3.1), the downward reserve request proportion ( $\chi_t^d$ ) is much  
472 higher than the upward reserve request proportion ( $\chi_t^u$ ), the ratio of which is close to 9:1 over the whole day.

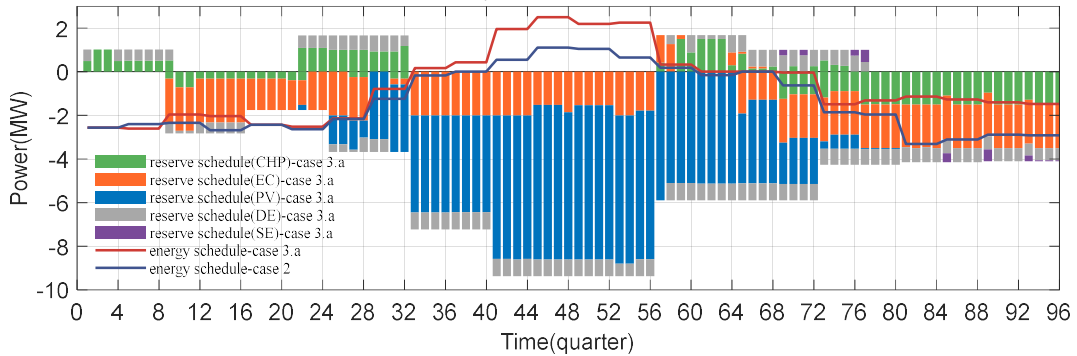


Fig.10 Day-ahead energy and reserve schedules of MEVPP in case 3.a

473  
474  
475  
476

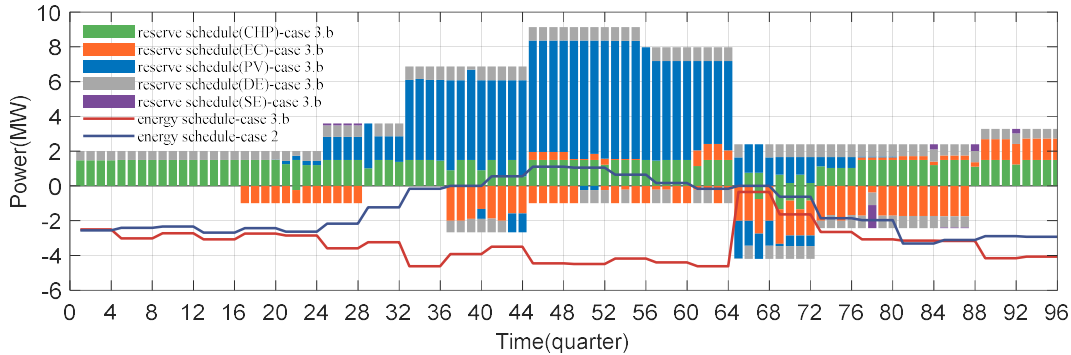
Tab.2 Costs of MEVPP in case 2 and case 3.a

	Case 2	Case 3.a
Day-ahead electricity cost $-\sum_t F_t^{DAM}$ (€)	3428.870	1994.153
Day-ahead natural gas cost $-\sum_t F_t^{GM}$ (€)	2904.966	3595.855
Upward reserve cost $-\sum_t \chi_t^u \cdot F_t^{ASM,u}$ (€)	--	-110.159
Downward reserve cost $\sum_t \chi_t^d \cdot F_t^{ASM,d}$ (€)	--	68.508
Electricity imbalance cost $\sum_t F_t^{EIP}$ (€)	-0.821	0
Unsupplied reserve penalty $\sum_t F_t^{URP}$ (€)	--	0
Natural gas imbalance cost $\sum_t F_t^{GIP}$ (€)	-2.140	-476.580
Start-up/shut-down & Operational cost $\sum_t CO_t^{sud} + CO_t^{op}$ (€)	1049.058	1050.586
<b>Total cost of MEVPP (€)</b>	<b>7379.933</b>	<b>6122.362</b>

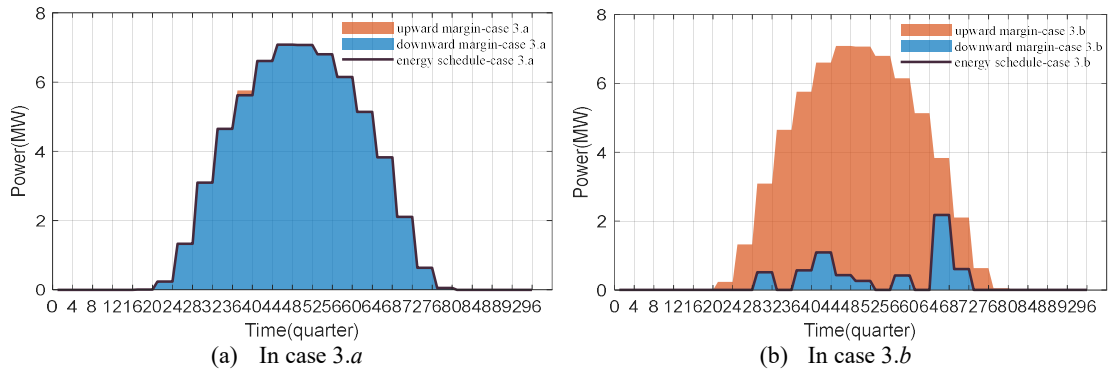
477 3.2.3 Case 3.a and case 3.b: Impacts of upward and downward reserve requests

478 The upward and downward reserve requests in case 3.a come from the data in reality, which are quite extreme.  
 479 The downward reserve request proportion ( $\chi_t^d$ ) is much higher than the upward reserve request proportion ( $\chi_t^u$ ),  
 480 the ratio of which is close to 9:1 over the whole day. To analyze the impacts of upward and downward reserve  
 481 requests, in case 3.b, the value of  $\chi_t^u$  in case 3.a is set to be the current value of  $\chi_t^d$ , and the value of  $\chi_t^d$  in case  
 482 3.a is set to be the current value of  $\chi_t^u$ .

483 The results of case 3.b are given in Fig.11, where MEVPP provides more upward reserve and less downward  
 484 reserve compared to Fig.10 of case 3.a. MEVPP decreases its day-ahead energy schedule throughout almost the  
 485 whole day to provide more upward reserve. Therefore, it can be received that the upward and downward reserve  
 486 requests can highly affect the MEVPP's behavior in upward and downward reserve services.



487 Fig.11 Day-ahead energy and reserve schedules of MEVPP in case 3.b  
 488



489 Fig.12 Day-ahead energy schedules of PV

490 It can also be observed from Fig.11 and Fig.10 that PV has a strong ability to provide upward and downward  
 491 reserves in the mid-day, especially during 8:15a.m.–16:00p.m. (quarter 33-64). To figure out the reason, the day-  
 492 ahead energy schedules of PV in both case 3.a and case 3.b are further given in Fig.12, together with their day-  
 493 ahead available capacities from which the technical capacity margins quantifying their ability to provide reserves  
 494 can be calculated. However, PV can only provide reserve in a limited period, 5:00a.m.–20:00p.m.(quarter 20-80),  
 495 constrained by solar radiation.  
 496

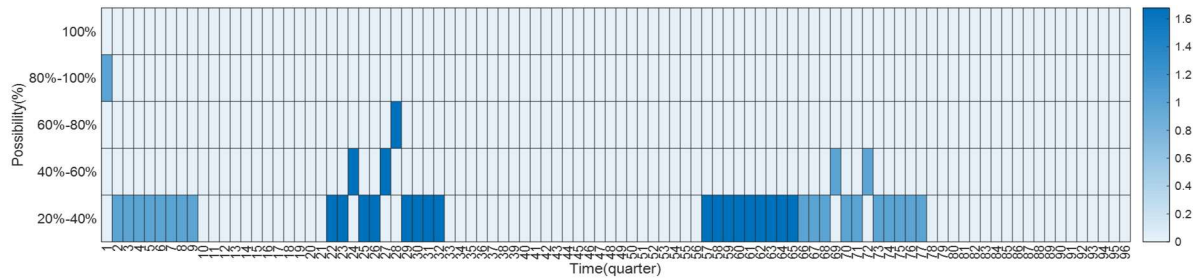
497 Moreover, in both two cases, the ability of SE to provide reserve is limited, as in Fig.10 and Fig.11. Because the  
 498 requirements of SE providing reserve are strict, as it is necessary for SE to provide a certain SOC level at the end of  
 499 the day considering reserve services. In this paper, to ensure that SE can provide the reserve deployment without  
 500 affecting its normal usage on the following day, the SOC value at the end of the day needs to go back to the initial  
 501 value (refer to Eq.(95)-(96)).  
 502

504 3.2.4 Case 3.a and case 3.b: Offer/bid strategy in ASM

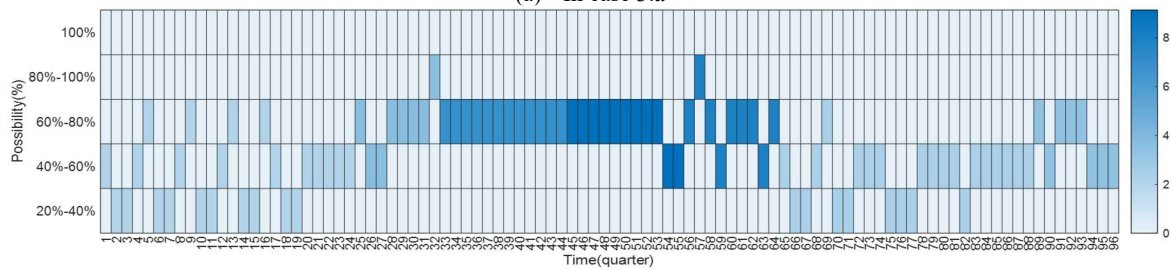
505 The day-ahead reserve schedules in Fig.10 and Fig.11 show the reserve quantities MEVPP offer/bid in ASM for  
 506 case 3.a and case 3.b, respectively. However, as is described in section 2.2.1, whether TSO accepts the offer/bid  
 507 depends on the offer/bid price of MEVPP under the pay-as-bid scheme. Fig.13 and Fig.14 present the offer and bid  
 508 price strategies MEVPP chooses each time in case 3.a and case 3.b, respectively. Y-axis shows the acceptance  
 509 probability of five price strategies. The corresponding price data of the five price strategies are given in Fig.3 and  
 510 Fig.4 in section 3.1. In Fig.13 and Fig.14, the darker the blue color is, the larger the offer/bid quantity is, this  
 511 is represented in scale by the palette table on the right side of the figures.  
 512

It can be observed that, in both Fig.13 and Fig.14 MEVPP offers/bids with quite low acceptance probability,

513 especially for the downward reserve. In Fig.14, the acceptance probability of MEVPP's bidding strategy is below  
 514 60% most of the time. This means that MEVPP prefers risky strategies in ASM. Higher profit is received if it offers  
 515 high price when selling upward reserve and bids low price when selling downward reserve, although the probability  
 516 of being accepted by TSO is low. Because the price of the offer (bid) is high (low) enough to compensate for the  
 517 low acceptance probability and generates profit. The downward reserve trading is even more risk preferred.  
 518 Because PV generator, which is one of the main downward reserve sources of MEVPP, has no fuel cost. Therefore,  
 519 under the current market rules that MEVPP needs to pay back a part of the money saved by the decreased  
 520 electricity production, PV has no reason to provide downward reserve if the price is higher than its operational cost,  
 521 which is 12€/MWh from Tab.S1 in **SUPPLEMENTARY MATERIAL**.  
 522

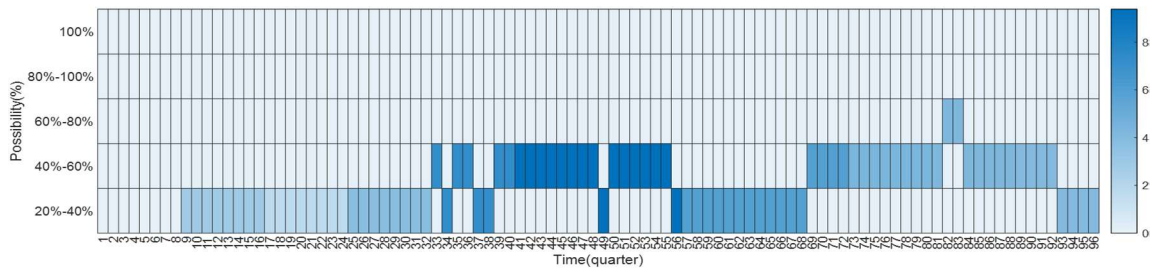


(a) In case 3.a

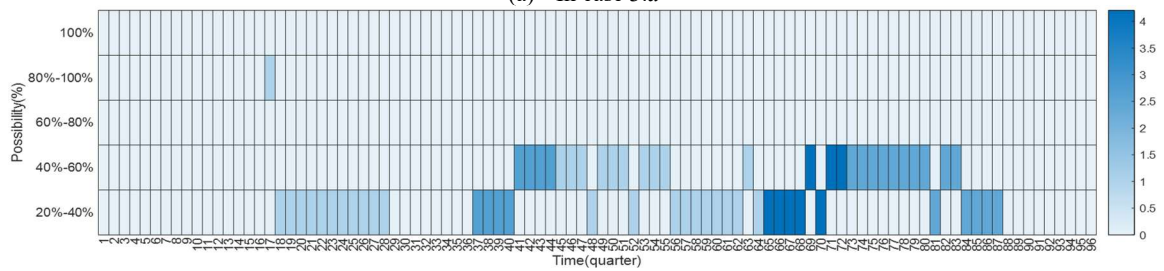


(b) In case 3.b

Fig.13 Offer price strategy for upward reserve MEVPP chooses each time



(a) In case 3.a



(b) In case 3.b

Fig.14 Bid price strategy for downward reserve MEVPP chooses each time

525  
526  
528  
529

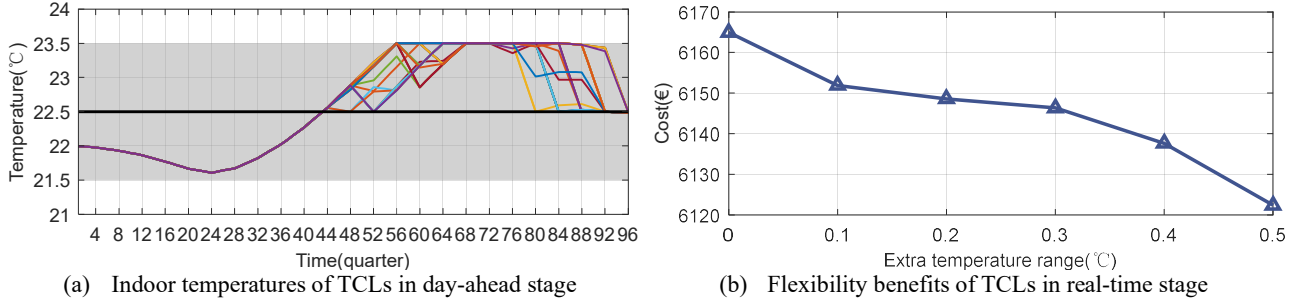
530  
531  
532  
533  
535  
536

### 537 3.2.5 Case 3.a and case 3.c: Impacts of non-electricity devices

538 The indoor temperatures of TCLs in the day-ahead energy schedule of case 3.a are given in Fig.15(a), where the  
 539 colorful curves represent the indoor temperatures of 30 TCLs. Before 11:00a.m. (quarter 44), TCLs do not consume  
 540 cooling because their indoor temperatures are lower than the satisfactory temperature represented by the black  
 541 curve in Fig.15(a). With the increase of the weather temperature given in Fig.8 in section 3.1, the indoor  
 542 temperature increases lagged and exceeds the satisfactory temperature at 11:00a.m., after when TCLs consume  
 543 cooling to reduce the indoor temperatures. Limited by the acceptable temperature range set by consumers'

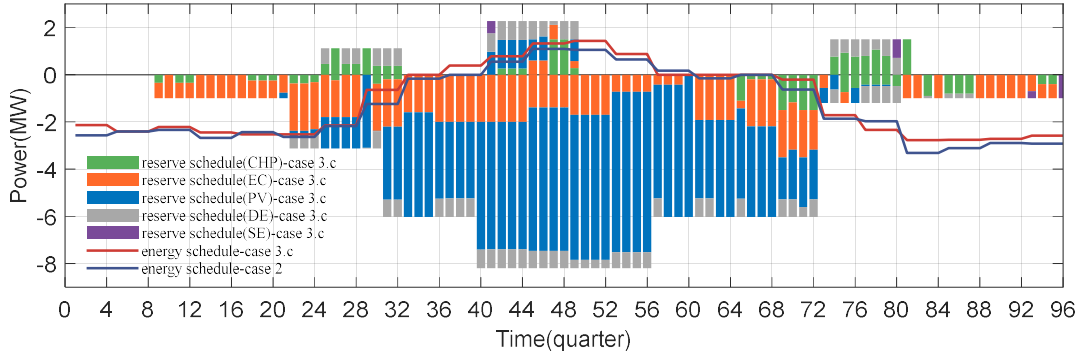
544 insensitivity and represented by the grey shadow in Fig.15(a), the indoor temperatures of all TCLs are kept within  
 545 22.5°C-23.5°C.

546 To analyze the economic achievements of the flexibility provided by TCLs, extra temperature range is set in the  
 547 real-time stage. In Fig.15(b), when the extra temperature range is 0°C, it means TCLs do not provide flexibility  
 548 service and all TCLs still range within 21.5°C-23.5°C in the real-time stage. When the extra temperature range is  
 549 0.5°C, it means TCLs can range within 21°C-24°C in the real-time stage, which is also applied by case 3.a. In  
 550 Fig.15(b), the cost of MEVPP decreases with the increase of extra temperature range. MEVPP can save the cost by  
 551 0.7%, from 6164.958€ to 6122.362€ through the flexibility provided by TCLs in case 3.a.  
 552



553 Fig.15 Indoor temperatures and flexibility benefits of TCLs in case 3.a

554 There exist non-electricity devices inside MEVPP that cannot provide reserve bands directly, including GB, AC,  
 555 and ST. To analyze their effects, in case 3.c, non-electricity devices are considered unavailable in the reserve  
 556 deployment, which means they cannot change their power profile during final dispatching. The results of case 3.c  
 557 are given in Fig.16. The reserves provided by CHP and EC decrease a lot compared with Fig.10. Because CHP and  
 558 EC couple electricity with natural gas and cooling, which need the support of non-electricity devices. Compared to  
 559 case 3.a, in case 3.c the total upward reserve of the entire day decreases by 24.1%, from 54.604MW to 41.422MW,  
 560 and the total downward reserve of the entire day decreases by 23.8%, from 468.148MW to 356.6320MW.  
 561 Therefore, although non-electricity devices cannot provide reserve bands directly, they can help other devices to  
 562 provide more reserve services. As in Tab.3, the total cost of MEVPP increases to 6778.620€, compared to  
 563 6122.362€ in case 3.a, which means that the use of non-electricity devices can save 9.7% of the cost for MEVPP.  
 564  
 565  
 566



568 Fig.16 Day-ahead energy and reserve schedules of MEVPP in case 3.c

569 Tab.3 Costs of MEVPP in case 3.a, case 3.c, case 3.d, case 3.e and case 4

570  
571  
572

	Case 3.a	Case 3.c	Case 3.d			Case 3.e			Case 4
Sub-scenario	-	-	2WM	4WM	0WM	240mins	480mins	0mins	-
Total cost of MEVPP(€)	6122.362	6778.620	6138.123	6188.408	6111.605	6144.863	6217.231	6089.811	6329.032

573  
 574 3.2.6 Case 3.a, case 3.d and case 3.e: Impacts of reserve regulations

575 The minimum offer/bid size and minimum delivery duration can impact the quality of the reserve service of  
 576 MEVPP. In case 3.a, the minimum offer/bid size is 1MW and the minimum delivery duration is 120mins given in  
 577 section 3.1. Case 3.d and case 3.e are set to analyze the impacts of these reserve regulations.

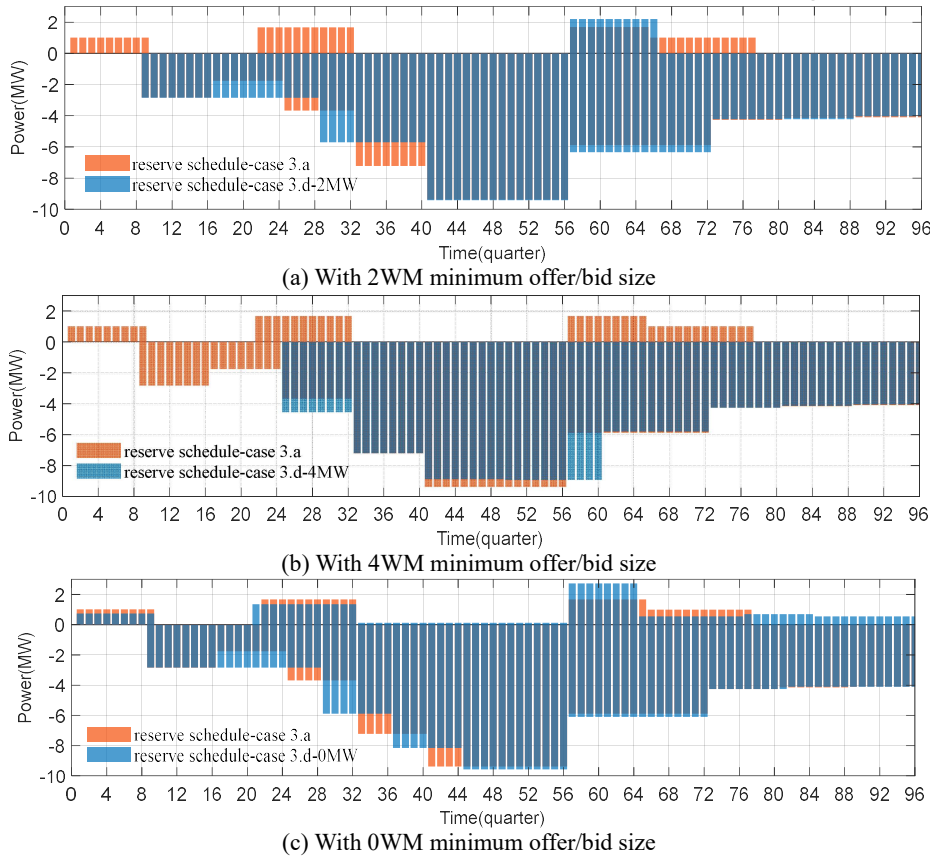
578 In case 3.d, the impacts of minimum offer/bid size on the reserve service are analyzed with the help of three sub-  
 579 scenarios set with different minimum offer/bid sizes:

580 When the minimum offer/bid size increases from 1MW to 2MW, the time when MEVPP provides upward  
 581 reserve decreases by 75.6% compared to case 3.a, as in Fig.17(a), however, with larger quantity because of the

582 higher minimum size constraint. The bars representing case 3.d are stacked before the bars representing case 3.a in  
 583 Fig.17. The cost of MEVPP increases by 0.3% from 6122.362€ to 6138.123€, as in Tab.3.

584 When the minimum offer/bid size keeps increasing to 4MW, MEVPP stops providing upward reserve, moreover,  
 585 downward reserve is not supplied during 2:15a.m.–6:00a.m.(quarter 9-24), as in Fig.17(b). Because for the upward  
 586 reserve during the whole day and downward reserve during 2:15a.m.–6:00a.m., enlarging the quantity to meet the  
 587 higher minimum size constraint is not profitable for MEVPP. The cost of MEVPP increases by 1.1% from  
 588 6122.362€ to 6188.408€ compared to case 3.a, as in Tab.3.

589 When the minimum offer/bid size decreases from 1MW to 0MW, MEVPP starts to provide upward reserve  
 590 during 8:15a.m.–14:00p.m.(quarter 33-56) and 19:30p.m.–24:00a.m.(quarter 78-96) compared to case 3.a in  
 591 Fig.17(c), however, with very small quantity. As in Tab.3, the cost of MEVPP decreases by 0.2% from 6122.362€  
 592 to 6111.605€. Decreasing the minimum offer/bid size can encourage more small-size reserve services, which makes  
 593 the reserve transaction more active. However, it also introduces difficulties for the management of TSO.



594  
595

596  
597

598  
599

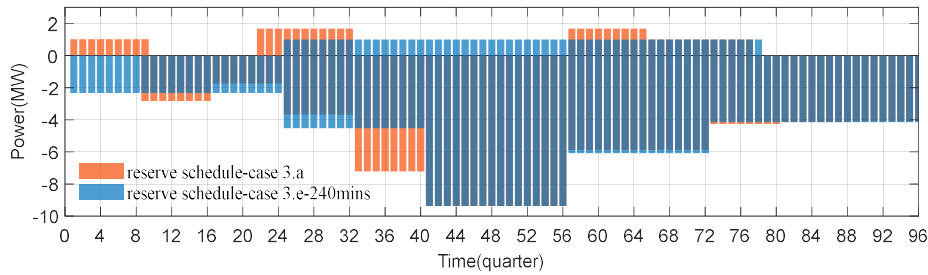
600  
601

602 In case 3.e, the impacts of minimum delivery duration on the reserve service are analyzed with the help of three  
 603 sub-scenarios set with different minimum delivery durations:

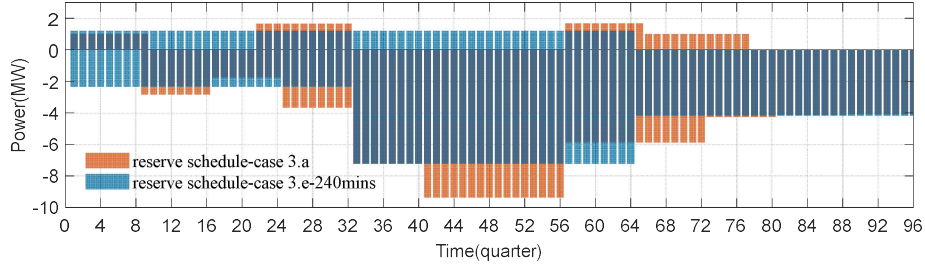
604 When the minimum delivery duration increases from 120mins in case 3.a to 240mins, the overall cost of MEVPP  
 605 increases by 0.4% from 6122.362€ to 6144.863€, as in Tab.3. Compared to case 3.a, the reserve service is flatter.  
 606 Under the longer minimum delivery duration constraint, the upward reserve is centralized to 6:15a.m.–  
 607 19:30p.m.(quarter 25-78) with a smaller uniform quantity value, and the downward reserve is provided throughout  
 608 the whole day, as in Fig.18(a). The bars representing case 3.e are stacked before the bars representing case 3.a in  
 609 Fig.18.

610 When the minimum delivery duration keeps increasing to 480mins as in Fig.18(b), MEVPP produces uniform  
 611 upward reserve quantity in a longer period. Also, the provided downward reserve is more stable. The total cost  
 612 increases by 1.6% to 6217.231€, compared to case 3.a, as in Tab.3.

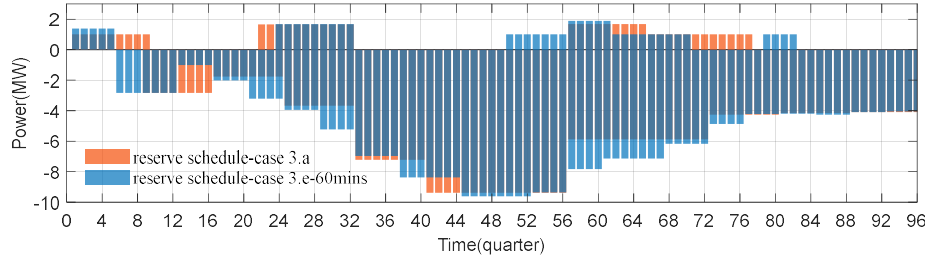
613 When the minimum delivery duration decreases from 120mins to 60mins, the overall cost of MEVPP decreases  
 614 by 0.5% from 6122.362€ to 6089.811€ compared to case 3.a, as in Tab.3. However, the quantities of both upward  
 615 and downward reserves are more fluctuated, as in Fig.18(c).



(a) With 240mins minimum delivery duration



(b) With 480mins minimum delivery duration



(c) With 60mins minimum delivery duration

Fig.18 Day-ahead reserve schedule of MEVPP in case 3.e

Above all, by different minimum offer/bid sizes and minimum delivery durations, TSO can receive reserve services from MEVPP with different qualities. When the regulations are adjusted within a reasonable range, such as in case 3.d and case 3.e, they have little impact on the cost of MEVPP. This means that TSO can obtain the required quality of reserve services through reasonable reserve regulations, which MEVPP is likely to be willing to accept because their impacts on the cost of MEVPP are quite little.

### 3.2.7 Case 3.a and case 4: Impacts of CM participation

Case 4 is set for analyzing the daily impacts of the CM contract, which is set in 4 continuous peak hours during 14:15 p.m.–18:00 p.m.(quarter 57-72) with the contracted capacity quantity 2 MW [8,9,11].

It can be observed from Fig.19 that the day-ahead energy schedule of MEVPP increases during 14:15 p.m.–15:00 p.m.(quarter 57-60) and the day-ahead upward reserve schedule increases during 15:15 p.m.–18:00 p.m.(quarter 61-72), compared to case 3.a, resulting from the constraints in the CM contract. The sum of provided energy and upward reserve during 14:15 p.m.–18:00 p.m.(quarter 57-72) increases by 43.9% from 23.264MW to 33.476MW compared to case 3.a, which can contribute to the energy supplying and system balancing during this peak period. As in Tab.3, the total cost of MEVPP increases by 3.4% from 6122.362€ to 6329.032€, which should be compensated by the CM remuneration, otherwise, MEVPP has no interest in participating in CM.

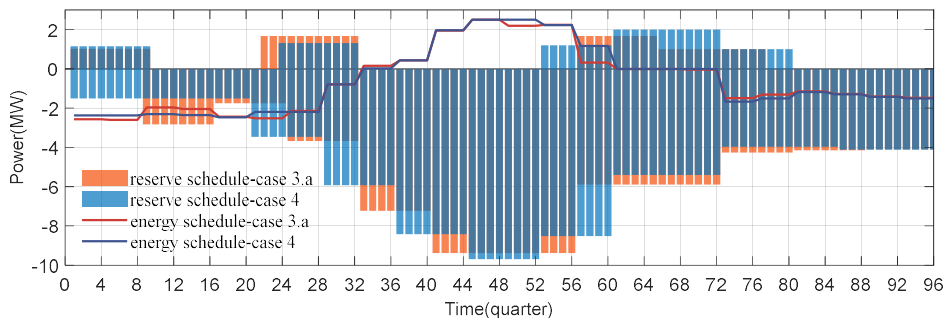


Fig.19 Day-ahead energy and reserve schedules of MEVPP in case 4

### 642 3.2.8 Discussion

643 The results of all the cases have been detailed analyzed and discussed in sections 3.2.1-3.2.7. This section  
644 reviews and summarizes the main achievements from the discussions of all the cases.

645 Case 1 and case 2 analyze the impacts of available PV capacity uncertainty. A higher budget of uncertainty  
646 comes with a conservative cost with less economic risk for MEVPP.

647 Case 2 and case 3.a analyze the impacts of ASM participation. MEVPP receives extra profit by trading reserves  
648 in ASM, which decreases the total cost of MEVPP by 17% in case 3.a compared to case 2.

649 Case 3.a and case 3.b analyze the impacts of upward and downward reserve requests, which highly affect the  
650 MEVPP's behavior in upward and downward reserve services. To maximize its profit, MEVPP chooses risky  
651 strategies in ASM in both cases. It offers (bids) high (low) price for upward (downward) reserve, although the  
652 corresponding acceptance probability is low.

653 Case 3.a and case 3.c analyze the impacts of non-electricity devices, which enhance the reserves provided by and  
654 the economic benefit of MEVPP. The provided upward and downward reserves are increased by 24.1% and 23.8%,  
655 respectively, and the total cost is reduced by 9.7% in case 3.a compared to case 3.c.

656 Case 3.a, case 3.d and case 3.e analyze the impacts of reserve regulations. The reserve quality provided by  
657 MEVPP can be guaranteed by setting reasonable reserve regulations, which have little impact on the cost of  
658 MEVPP. Therefore, MEVPP is likely to be willing to accept the given regulations.

659 Case 3.a and case 4 analyze the impacts of CM participation. Taking part in CM contributes to the capacity  
660 adequacy of the power system. However, the total cost of MEVPP is increased by 3.4% from 6122.362€ in case 3.a  
661 to 6329.032€ in case 4, which should be compensated by the CM remuneration.

## 662 4. Conclusion

663 In this study, an optimal energy and reserve scheduling model of a MEVPP is developed. The coordination of  
664 energy and reserve services is realized by following the developed holistic market framework. With the help of  
665 numerical analysis, there are some main conclusions achieved from the perspectives of MEVPP and TSO:

666 From the perspective of MEVPP: (1) MEVPP can receive extra profit by trading reserves in ASM. In the case  
667 study, it helps MEVPP decrease its total cost by 17%. (2) Non-electricity devices can increase the reserves provided  
668 by MEVPP, which improves the flexibility and further enhances the economic profit of MEVPP. The provided  
669 reserves are increased by about 24% in both directions, and the total cost is reduced by 9.7% in the numerical  
670 analysis. (3) Under the current market situation, MEVPP prefers risky strategies in ASM. To maximize its profit,  
671 MEVPP always chooses high (low) offer (bid) price for upward (downward) reserve with low acceptance  
672 probability.

673 From the perspective of TSO: (1) MEVPP can be a promising reserve service supplier for TSO. Because  
674 reasonable reserve regulations can improve the quality of the reserves provided by MEVPP to TSO, however, with  
675 only little impact on the cost of MEVPP. (2) MEVPP would take part in CM to ensure the capacity adequacy of the  
676 power system if the remuneration given is higher than the cost loss for following the contract set by TSO.

## 677 CRedit authorship contribution statement

678 **Jian Wang:** Conceptualization, Methodology, Formal analysis, Software, Validation, Writing - original draft.

679 **Valentin Ilea:** Methodology, Investigation, Writing - review & editing, Visualization. **Cristian Bovo:**  
680 Conceptualization, Resources, Supervision. **Ning Xie:** Conceptualization, Resources, Supervision. **Yong Wang:**  
681 Writing - review & editing.

## 682 Acknowledgements

683 This work was supported by China Scholarship Council.

## 684 Appendix A

685 The first kind is the linearization of the maximum functions inserted in constraints (41) and (42), as is given in (A.1) and (A.2),  
686 respectively. Auxiliary continuous variables  $p_{vpp,t}^{DA-RT}$  and  $p_{vpp,t}^{RT-DA}$ , and auxiliary binary variables  $x_{vpp,t}^{u,A}$  and  $x_{vpp,t}^{d,A}$  are introduced to help the  
687 linearization.  $M_1$  is a big enough value, following the rule:  $M_1 \square M$ .  
688

$$\begin{cases}
A_{vpp,t}^{RT,u} + p_{vpp,t}^{URP,u} \geq p_{vpp,t}^{DA-RT} + \sum_{w \in W_u} A_{vpp,t,w}^{DA,u} \\
p_{vpp,t}^{DA-RT} \geq p_{vpp,t}^{DA} - p_{vpp,t}^{RT} - (1 - \sum_{w \in W_u} I_{vpp,t,w}^u) \cdot M \\
p_{vpp,t}^{DA-RT} \geq 0 \\
p_{vpp,t}^{DA-RT} \leq p_{vpp,t}^{DA} - p_{vpp,t}^{RT} - (1 - \sum_{w \in W_u} I_{vpp,t,w}^u) \cdot M + (1 - x_{vpp,t}^{u,A}) \cdot M_1 \\
p_{vpp,t}^{DA-RT} \leq 0 + x_{vpp,t}^{u,A} \cdot M_1
\end{cases} \quad (A.1)$$

$$\begin{cases}
A_{vpp,t}^{RT,d} + p_{vpp,t}^{URP,d} \geq p_{vpp,t}^{RT-DA} + \sum_{w \in W_d} A_{vpp,t,w}^{DA,d} \\
p_{vpp,t}^{RT-DA} \geq p_{vpp,t}^{RT} - p_{vpp,t}^{DA} - (1 - \sum_{w \in W_d} I_{vpp,t,w}^d) \cdot M \\
p_{vpp,t}^{RT-DA} \geq 0 \\
p_{vpp,t}^{RT-DA} \leq p_{vpp,t}^{RT} - p_{vpp,t}^{DA} - (1 - \sum_{w \in W_d} I_{vpp,t,w}^d) \cdot M + (1 - x_{vpp,t}^{d,A}) \cdot M_1 \\
p_{vpp,t}^{RT-DA} \leq 0 + x_{vpp,t}^{d,A} \cdot M_1
\end{cases} \quad (A.2)$$

689  
690  
691  
692  
693

The second kind is the multiplier of a binary variable ( $I_{dc,t}^{S1}$ ) and a continuous variable ( $D_{dc,t}^{S1}$ ), which is in Eq.(73). Eq.(73) is linearized together with Eq.(74), with the help of an auxiliary binary variable  $x_{dc,t}^{S1,A}$ .  $M$  is a big enough value. Eq.(73)-(74) are converted to (A.3):

$$\begin{cases}
\theta_{dc,t}^{S1} = a_{dc} \cdot \theta_{dc,t-1}^{S1} + (1 - a_{dc}) \cdot (\theta_t^o - R_{dc} \cdot D_{dc,t}^{S1}) \\
-(1 - x_{dc,t}^{S1,A}) \cdot M \leq \theta_{dc,t}^{S1} - \theta_{dc,t}^{S1,sa} \leq x_{dc,t}^{S1,A} \cdot M \\
0 \leq D_{dc,t}^{S1} \leq x_{dc,t}^{S1,A} \cdot M
\end{cases} \quad (A.3)$$

694  
695  
696

The third kind is the incompatibility of two variables ( $A_{se,t}^{S2,u}$  and  $A_{se,t}^{S2,d}$ ) in Eq.(95). It is linearized in (A.4) by introducing an auxiliary binary variable  $x_{se,t}^{S2,A}$ :

$$\begin{cases}
0 \leq A_{se,t}^{S2,u} \leq x_{se,t}^{S2,A} \cdot M \\
0 \leq A_{se,t}^{S2,d} \leq (1 - x_{se,t}^{S2,A}) \cdot M
\end{cases} \quad (A.4)$$

698

## Reference

- 699 [1] [https://ec.europa.eu/info/strategy/priorities-2019-2024/european-green-deal\\_en](https://ec.europa.eu/info/strategy/priorities-2019-2024/european-green-deal_en).  
700 [2] [https://www.ndrc.gov.cn/wsdwhfz/202111/t20211111\\_1303691\\_ext.html](https://www.ndrc.gov.cn/wsdwhfz/202111/t20211111_1303691_ext.html).  
701 [3] C. Wang and J. Song, "Performance assessment of the novel coal-fired combined heat and power plant integrating with flexibility  
702 renovations," *Energy*, vol. 263, p. 125886, 2023.  
703 [4] R. Yan, J. Wang, S. Huo, J. Zhang, S. Tang, and M. Yang, "Comparative study for four technologies on flexibility improvement  
704 and renewable energy accommodation of combined heat and power system," *Energy*, vol. 263, p. 126056, 2023.  
705 [5] V. Mladenov, V. Chobanov, E. Zafeiropoulos, and V. Vita, "Characterisation and evaluation of flexibility of electrical power  
706 system," in *2018 10th Electrical Engineering Faculty Conference (Bulef)*, 2018: IEEE, pp. 1-6.  
707 [6] E. Zafeiropoulos *et al.*, "Smart grid flexibility solutions for transmission networks with increased RES penetration," *Proceedings  
708 of the CIGRE Paris Session*, p. 10711, 2022.  
709 [7] V. Vita, C. Christodoulou, I. Zafeiropoulos, I. Gonos, M. Asprou, and E. Kyriakides, "Evaluating the flexibility benefits of smart  
710 grid innovations in transmission networks," *Applied Sciences*, vol. 11, no. 22, p. 10692, 2021.  
711 [8] Italian Regulatory Authority for Energy, Networks and Environment (ARERA), Consultation Document 422/2018/R/eel, 2 Aug.  
712 2018, available online: <https://www.arera.it/it/docs/18/422-18.htm>.  
713 [9] Italian Transmission System Operator (Terna S.p.A.), "Regulation governing the methods for creation, qualification and  
714 managements of enabled mixed virtual units (UVAM) to the Ancillary service market", 25 Sept. 2018, available online:  
715 <https://download.terna.it/terna/0000/1071/84.PDF>.  
716 [10] V. Mladenov *et al.*, "A flexibility market platform for electricity system operators using blockchain technology," *Energies*, vol. 15,  
717 no. 2, p. 539, 2022.  
718 [11] F. Gulotta *et al.*, "Opening of the Italian Ancillary Service Market to Distributed Energy Resources: Preliminary Results of  
719 UVAM project," in *2020 IEEE 17th International Conference on Smart Communities: Improving Quality of Life Using ICT, IoT  
720 and AI (HONET)*, 2020: IEEE, pp. 199-203.  
721 [12] Italian Regulatory Authority for Energy, Networks and Environment (ARERA), Consultation Document 3 June 2020,  
722 201/2020/R/eel, available online: [www.arera.it/it/docs/20/20-20.htm](http://www.arera.it/it/docs/20/20-20.htm).  
723 [13] M. Rekik, Z. Chtourou, N. Mitton, and A. Atieh, "Geographic routing protocol for the deployment of virtual power plant within  
724 the smart grid," *Sustainable Cities and Society*, vol. 25, pp. 39-48, 2016.  
725 [14] M. Shafiekhani, A. Ahmadi, O. Homaei, M. Shafie-khah, and J. P. Catalão, "Optimal bidding strategy of a renewable-based  
726 virtual power plant including wind and solar units and dispatchable loads," *Energy*, vol. 239, p. 122379, 2022.  
727 [15] S. Wang and W. Wu, "Aggregate flexibility of virtual power plants with temporal coupling constraints," *IEEE Transactions on  
728 Smart Grid*, vol. 12, no. 6, pp. 5043-5051, 2021.

- 729 [16] N. Pourghaderi, M. Fotuhi-Firuzabad, M. Moeini-Aghaie, and M. Kabirifar, "Commercial demand response programs in bidding  
730 of a technical virtual power plant," *IEEE Transactions on Industrial Informatics*, vol. 14, no. 11, pp. 5100-5111, 2018.
- 731 [17] Y. Zhang, F. Liu, Z. Wang, Y. Su, W. Wang, and S. Feng, "Robust scheduling of virtual power plant under exogenous and  
732 endogenous uncertainties," *IEEE Transactions on Power Systems*, vol. 37, no. 2, pp. 1311-1325, 2021.
- 733 [18] A. Baringo, L. Baringo, and J. M. Arroyo, "Day-ahead self-scheduling of a virtual power plant in energy and reserve electricity  
734 markets under uncertainty," *IEEE Transactions on Power Systems*, vol. 34, no. 3, pp. 1881-1894, 2018.
- 735 [19] W. Chen, J. Qiu, J. Zhao, Q. Chai, and Z. Y. Dong, "Bargaining game-based profit allocation of virtual power plant in frequency  
736 regulation market considering battery cycle life," *IEEE Transactions on Smart Grid*, vol. 12, no. 4, pp. 2913-2928, 2021.
- 737 [20] J. Naughton, H. Wang, M. Cantoni, and P. Mancarella, "Co-optimizing virtual power plant services under uncertainty: a robust  
738 scheduling and receding horizon dispatch approach," *IEEE Transactions on Power Systems*, vol. 36, no. 5, pp. 3960-3972, 2021.
- 739 [21] H. Zhao *et al.*, "Active dynamic aggregation model for distributed integrated energy system as virtual power plant," *Journal of  
740 Modern Power Systems and Clean Energy*, vol. 8, no. 5, pp. 831-840, 2020.
- 741 [22] L. B. Khouzestani, M. K. Sheikh-El-Eslami, A. H. Salemi, and I. G. Moghaddam, "Virtual smart energy Hub: A powerful tool for  
742 integrated multi energy systems operation," *Energy*, vol. 265, p. 126361, 2023.
- 743 [23] L. Fan, D. Ji, G. Lin, P. Lin, and L. Liu, "Information gap-based multi-objective optimization of a virtual energy hub plant  
744 considering a developed demand response model," *Energy*, p. 127462, 2023.
- 745 [24] N. Good and P. Mancarella, "Flexibility in multi-energy communities with electrical and thermal storage: A stochastic, robust  
746 approach for multi-service demand response," *IEEE Transactions on Smart Grid*, vol. 10, no. 1, pp. 503-513, 2017.
- 747 [25] Y. Zhou, Z. Wei, G. Sun, K. W. Cheung, H. Zang, and S. Chen, "A robust optimization approach for integrated community energy  
748 system in energy and ancillary service markets," *Energy*, vol. 148, pp. 1-15, 2018.
- 749 [26] H. Zhao, B. Wang, Z. Pan, H. Sun, Q. Guo, and Y. Xue, "Aggregating additional flexibility from quick-start devices for multi-  
750 energy virtual power plants," *IEEE Transactions on Sustainable Energy*, vol. 12, no. 1, pp. 646-658, 2020.
- 751 [27] S. Bahramara, S. Shahrokhi, P. Sheikahmadi, R. Khezri, and S. Muyeen, "Modeling the risk-based decisions of the microgrid in  
752 day-ahead energy and reserve markets considering stochastic dispatching of electrical and thermal energy storages," *Energy  
753 Conversion and Management: X*, vol. 14, p. 100201, 2022.
- 754 [28] M. Vanouni and N. Lu, "A reward allocation mechanism for thermostatically controlled loads participating in intra-hour ancillary  
755 services," *IEEE Transactions on Smart Grid*, vol. 9, no. 5, pp. 4209-4219, 2017.
- 756 [29] Z. Yi, Y. Xu, W. Gu, and W. Wu, "A multi-time-scale economic scheduling strategy for virtual power plant based on deferrable  
757 loads aggregation and disaggregation," *IEEE Transactions on Sustainable Energy*, vol. 11, no. 3, pp. 1332-1346, 2019.
- 758 [30] M. Vahedipour-Dahraie, H. Rashidizadeh-Kermani, M. Shafie-Khah, and J. P. Catalão, "Risk-averse optimal energy and reserve  
759 scheduling for virtual power plants incorporating demand response programs," *IEEE Transactions on Smart Grid*, vol. 12, no. 2,  
760 pp. 1405-1415, 2020.
- 761 [31] M. Khojasteh, P. Faria, and Z. Vale, "A robust model for aggregated bidding of energy storages and wind resources in the joint  
762 energy and reserve markets," *Energy*, vol. 238, p. 121735, 2022.
- 763 [32] M. Z. Oskouei, B. Mohammadi-Ivatloo, M. Abapour, M. Shafiee, and A. Anvari-Moghaddam, "Strategic operation of a virtual  
764 energy hub with the provision of advanced ancillary services in industrial parks," *IEEE Transactions on Sustainable Energy*, vol.  
765 12, no. 4, pp. 2062-2073, 2021.
- 766 [33] Y. Mu, C. Wang, Y. Cao, H. Jia, Q. Zhang, and X. Yu, "A CVaR-based risk assessment method for park-level integrated energy  
767 system considering the uncertainties and correlation of energy prices," *Energy*, vol. 247, p. 123549, 2022.
- 768 [34] <https://www.terna.it/en/electric-system/capacity-market>.
- 769 [35] F. Castellani, "Distributed Energy Resources: a new asset for ancillary services market," 2018.
- 770 [36] N. Mazzi, J. Kazempour, and P. Pinson, "Price-taker offering strategy in electricity pay-as-bid markets," *IEEE Transactions on  
771 Power Systems*, vol. 33, no. 2, pp. 2175-2183, 2017.
- 772 [37] D. J. Swider, "Simultaneous bidding in day-ahead auctions for spot energy and power systems reserve," *International Journal of  
773 Electrical Power & Energy Systems*, vol. 29, no. 6, pp. 470-479, 2007.
- 774 [38] <https://www.mercatoelettrico.org/En/default.aspx>.
- 775 [39] <https://www.terna.it/en/electric-system/transparency-report>.
- 776 [40] <https://www.arpalombardia.it/Pages/Meteorologia/Richiesta-dati-misurati.aspx>.
- 777 [41] D. S. Callaway, "Tapping the energy storage potential in electric loads to deliver load following and regulation, with application  
778 to wind energy," *Energy Conversion and Management*, vol. 50, no. 5, pp. 1389-1400, 2009.
- 779